Developmental Biology 445 (2019) 256–270

Contents lists available at ScienceDirect

Developmental Biology

journal homepage: www.elsevier.com/locate/developmentalbiology

Dual embryonic origin of the mammalian enteric nervous system

Irina Brokhman[a,*,1], Jie Xu[a,1], Brenda L.K. Coles[a], Rozita Razavi[a], Silvia Engert[b], Heiko Lickert[b], Robert Babona-Pilipos[c], Cindi M. Morshead[d], Eric Sibley[e], Chin Chen[f], Derek van der Kooy[a,*]

[a] Department of Molecular Genetics, University of Toronto, Ontario M5S 1A8, Canada
[b] Helmholtz Zentrum München, Institute of Diabetes and Regeneration Research, 85764 Neuherberg, Germany
[c] Institute of Biomaterials and Biomedical Engineering", University of Toronto, Ontario M5S 3E1, Canada
[d] Department of Surgery, Division of Anatomy, University of Toronto, Ontario M5S 1A8, Canada
[e] Division of Pediatric Gastroenterology, Stanford University School of Medicine, Palo Alto, CA 94304, USA
[f] Department of Pediatrics, Stanford University School of Medicine, Stanford, CA 94305-5208, USA

ARTICLE INFO

Keywords:
Enteric nervous system
Lineage tracing
Neural crest
Pdx1-Cre-derived neural progenitors
Duodenum
Pancreas

ABSTRACT

The enteric nervous system is thought to originate solely from the neural crest. Transgenic lineage tracing revealed a novel population of clonal pancreatic duodenal homeobox-1 (Pdx1)-Cre lineage progenitor cells in the tunica muscularis of the gut that produced pancreatic descendants as well as neurons upon differentiation in vitro. Additionally, an in vivo subpopulation of endoderm lineage enteric neurons, but not glial cells, was seen especially in the proximal gut. Analysis of early transgenic embryos revealed Pdx1-Cre progeny (as well as Sox-17-Cre and Foxa2-Cre progeny) migrating from the developing pancreas and duodenum at E11.5 and contributing to the enteric nervous system. These results show that the mammalian enteric nervous system arises from both the neural crest and the endoderm. Moreover, in adult mice there are separate Wnt1-Cre neural crest stem cells and Pdx1-Cre pancreatic progenitors within the muscle layer of the gut.

1. Introduction

The enteric nervous system (ENS) provides an intrinsic innervation of the gastrointestinal tract and controls the peristaltic and secretory functions of the gut wall (Bayliss and Starling, 1899). The mammalian ENS is composed of several neuronal subtypes and enteric glia organized in ganglionic plexi (the myenteric (Auerbach's) and submucosal (Meissner's) plexi (Furness and Costa, 1980). Anatomically, the submucosal plexus (SP) is situated throughout the submucosal space between the circular muscle layer (CML) and the gut epithelium itself, whereas the myenteric plexus (MP) is located between the circular and longitudinal muscle layers (LML) of the tunica muscularis (TM) (Costa et al., 2000) (Fig. 1A). In the mammalian intestine most enteric neurons involved in the regulation of gut motility are located in the MP, whereas submucosal neurons primarily regulate secretion and vascular tone (Costa et al., 2000). Considerable evidence has shown that the mammalian and avian ENS originate from ectodermal neural crest (NC) cells (Yntema and Hammond, 1954; Le Douarin, 1969; Le Douarin and Dupin, 1993; Durbec et al., 1996). In early embryogenesis NC cells migrate throughout the developing embryo, reach the developing gut at E9.5 in mice and begin to form ENS (Durbec et al., 1996), although the gut contractions that are seen first at E13.5 in mouse are of myogenic origin only (Roberts et al., 2010).

Similarities between pancreatic β-cells and neurons have been noted since the end of the last century (Pearse, 1982), and pancreatic endocrine cells were suggested in some early studies to be of NC origin (Pearse and Polak, 1971). Nevertheless, several transplantation and lineage tracing experiments have demonstrated clearly the endodermal origin of the pancreas (Pictet et al., 1976; Andrew et al., 1983, 1998; Fontaine and Le Douarin, 1977; Jonsson et al., 1994). The established concept of the ectodermal origin of neural cells has been challenged by observations of unexpected patterns of neurogenesis in non-vertebrate organisms; some of the foregut neurons of the sea urchin develop from the endoderm and the ENS of the sea anemone is generated by both ectoderm and endoderm (Wei et al., 2011; Nakanishi et al., 2012). Endodermal neurogenesis in mammals was first suggested by the isolation of single, rare stem cells from the adult mouse pancreas, that gave rise to differentiated pancreatic cell types, as well as to separate neuronal progeny, in vitro and in vivo (Seaberg et al., 2004; Smukler et al., 2011). Indeed, evolutionary hypotheses suggest that at least portions of both the neuronal and pancreatic developmental programs are controlled by the same master transcription factor regulators

* Corresponding authors.
E-mail addresses: ira.brokhman@gmail.com (I. Brokhman), derek.van.der.kooy@utoronto.ca (D. van der Kooy).
[1] These authors made an equal contribution to this work.

https://doi.org/10.1016/j.ydbio.2018.11.014
Received 29 September 2017; Received in revised form 21 November 2018; Accepted 21 November 2018
Available online 22 November 2018

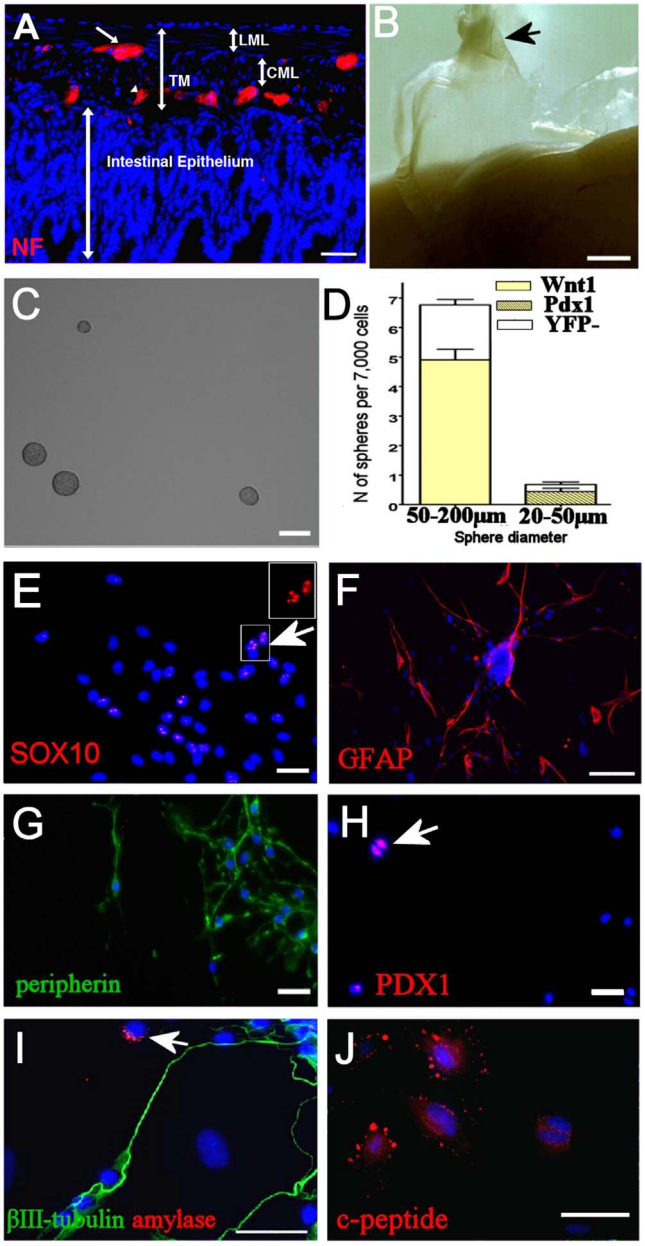

Fig. 1. Different size colonies with distinct development potentials are formed by progenitors residing in the TM of adult gut. (**A**) Immunostaining for neurofilament (NF) in adult intestine shows the topography of the ENS: a neuron in the SP (submucosal plexus) is indicated with an arrowhead and in the MP (myenteric plexus) with an arrow. TM (tunica muscularis), LML (longitudinal muscle layer), CML (circular muscle layer). (**B**) Microphotography of the TM surgical dissection. The dissection isolates specifically the longitudinal muscle layer and myenteric plexus layer of the TM. (**C**) Gut TM contains multipotent cells that form spheres with different diameters. (**D**) Analyses of the frequencies of clonal sphere numbers (per 7000 cells after 7 days of culturing) from separate Pdx1-Cre and Wnt1-Cre mouse lineages in the TM from throughout the gut (as well as spheres not accounted for by either lineage; YFP- in the case of each of the separate transgenic mouse strains) in small and large diameter bins. Data represent means ± SEMs, n = 3 mice per stain with 72 wells counted for each strain (from 24 well plates). (**E - J**) Immunohistochemistry analysis of development potential of TM-derived spheres (**E - G**) 50–200 µm diameter spheres reveals that they can be induced to differentiate into cells that express specific markers normally associated with neural crest progeny: (**E**) SOX10 expressing cells, inset shows single red channel, (**F**) GFAP+ glial cells (red), (**G**) peripherin+ neurons (green). (**H-I**) 20–50 µm diameter spheres produce cells that can be induced to differentiate into cells that express specific markers normally associated with pancreatic cell type progeny: (**H**) PDX1-expressing cells (red), (**I**) amylase+ cells (red) as well as ßIII-tubulin+ (green) neuronal progeny, (**J**) c-peptide+ cells (red) (**I,J**). Cell nuclei were counterstained with Hoechst stain (blue). Scale bars: (**A,E,H,I**) = 20 µm, (**B**) = 1 cm, (**C**) = 150 µm, (**F,J**) = 100 µm, (**G**) = 50 µm.

(Arntfield and van der Kooy, 2011), such as Pax6, Pax4, Isl1, NeuroD/2, Nkx2.2 (Edlund, 2002), Islet-1, Hb9 (Vult von Steyern et al., 1999).

Adult stem cells are usually limited to producing the cell types of their tissue of origin, and represent unique systems for studying the processes of development. However, given that endodermal-derived pancreatic stem cells give rise to such presumed ectodermal derivatives as neurons, we asked whether any neurons of the mammalian ENS also might be derived from the endoderm. Taking advantage of genetically defined lineage tracing approaches, we found that the TM of the adult mouse gut contains previously unidentified clonal multipotent progenitor cells from the pancreatic lineage, as well as pancreatic lineage marked neurons. Due to the limited self-renewal potential of this new population of pancreatic-derived multipotent cells in vitro, we consider them to be progenitors (Seaberg and van der Kooy, 2003). These findings lead to the surprising conclusion that the ENS arises from both NC and endoderm sources that may share similar developmental programs.

2. Materials and methods

Mice used in this from D.Melton, now available from Jackson; RRID: IMSR_JAX:02968), Wnt1-Cre (gift from A. McMahon), Rosa-YFP/R26R-EYFP (Jackson labs; RRID: IMSR_JAX:006148), Pdx1$^{Flox/Flox}$; RRID: IMSR_JAX:030177, CD1 (Charles River; RRID: IMSR_CRL:22), Foxa2$^{tm2.1(cre/Esr1)Moon/J}$(Jackson labs; RRID: IMSR_JAX:008335), Sox17-2A-iCre (abbreviated as Sox17-Cre; MGI:4418897), ROSAmT/mG (MGI: RRID: IMSR_MGI:4418909), Rosa-CAG-TdTomato/Ai14 (abbreviated as TdRed, Jackson labs; RRID: IMSR_JAX:007914). Mice homozygous for the floxed Pdx1 allele were generated as previously described (Chen et al., 2009).

2.1. Tamoxifen administration

99 mg of tamoxifen (Sigma) was dissolved by sonication in a solution of 100 µl of ethanol (Sigma) and 1 ml of peanut seed oil (Sigma). The solution was kept in a ~50 °C water bath during preparation and prior to administration to avoid precipitation. 50 µl doses of this solution were administered to pregnant mothers by oral gavage. All animal studies were approved by the Office of Research Ethics and Animal Care Committee at the University of Toronto. For staging, embryos were assumed to be 0.5 dpc at noon on the morning a vaginal plug was found.

2.2. Cell culture

Isolation of enteric precursor cells was performed separately for duodenum, ileum and colon of 10-weeks old mice as previously described (Schäfer et al., 1997; Estrada-Mondaca et al., 2007). Briefly, the longitudinal muscle layer was lifted carefully and separated from underlying circular muscle and mucosal layers along one end of the gut segment by teasing the layers apart with fine tweezers to avoid excessive stretching. In many of the gut segments, the outer muscle layer could be peeled off like a sleeve. This micro-dissected tissue contained longitudinal smooth muscle sheets with the attached myenteric ganglia. These longitudinal muscle and myenteric ganglia portions of the TM segments then were incubated in 0.025% trypsin/EDTA (Gibco,25300-054) plus 1 mg/ml type 4 collagenase (Gibco) in Ca, Mg-free HBSS for 30 min at 37 °C and triturated with a small-borehole siliconized pipette into a single cell suspension. The digestion was quenched with two volumes of serum-free medium (see below). Larger tissue segments were removed after a short period of sedimentation and centrifugation was performed for 5 min at 200*g* and 20 °C. Cells were counted using Trypan Blue exclusion and immediately plated at a density of 7, 000 cells per well in 24 well plate (Corning) (7cells /1 µl) in a volume of 1 ml defined SFM (Tropepe et al., 1999) containing 1x B27 (Gibco-BRL), 10 ng/ml FGF2 (Sigma), 20 ng/ml EGF (Sigma)

and 2 μg/ml heparin (Sigma) in 24-well uncoated plates (BD Biosciences) for 1 week without moving to decrease the incidence of non-clonal colonies (Coles-Takabe et al., 2008) It is important to mention that in these culture conditions we found that 12 ± 1.5% of TM derived colonies were arising by multicellular aggregation (see below).

Following similar TM tissue segment isolations, other cells were FACS sorted and plated on Matrigel for differentiation assays or for RT-PCR (see below).

2.3. Clonal and non-clonal colony formation from TM of Pdx1-Cre x Rosa-YFP mice

In order to estimate the proportions of YFP+ (Pdx1 lineage) versus YFP- clonal spheres above, we rejected any wells that contained mixed non-clonal spheres from all further experimental analyses. The Pdx1-Cre progeny were generated exclusively by YFP+ clonal Pdx1 lineage spheres. Immunostaining with anti-GFP antibody (which recognizes both GFP and YFP proteins) revealed the complete absence of GFP staining in the cells differentiated from YFP- spheres, whereas all of the cells from YFP+ spheres expressed reporter protein, confirming the clonality of all of the analyzed samples (data not shown). Further data supporting the hypothesis that the pancreatic spheres take origin from single cells comes similar mixing experiments employing marked and unmarked pancreatic cells, and from single cell per well experiments where 0.03% of single pancreatic cells in 96 well plates formed clonal spheres – a frequency close to the 0.02% frequency of sphere forming cells when pancreatic cells were cultured at 20 cells/μl. (Seaberg et al., 2004). Individual spheres were transferred to wells coated with Matrigel basement membrane matrix (0.6 mg/ml, Becton-Dickinson) in SFM containing 1% fetal bovine serum and grown for an additional 1 week for the assay of differentiated cells. For single sphere passaging individual colonies were dissociated with Trypsin-EDTA for 5 min at 37 °C, 5 min at room temperature, triturated with siliconized small-borehole glass pipettes and re-plated at the indicated cell density in the SFM media (described above) for 1 week.

2.4. Fluorescence activated cell sorting (FACS)

Dissociated TM cells were sorted based on YFP expression with a FACSAria System (BD Biosciences). Gating criteria for the analysis of YFP-expressing cells were set according to the level of autofluorescence of non-fluorescent controls from Rosa-YFP alone animals.

2.5. Immunohistochemistry

Gut tissue were fixed in 4% paraformaldehyde overnight and equilibrated for 24 h in 30% sucrose. Samples were then embedded in cryoprotectant (Ted Pella), sectioned (12–15 μm thick) using a Jencons OTF5000 cryostat, and mounted on Superfrost Plus slides (Fisher Scientific). Staining was performed following microwave antigen retrieval (Shi et al., 1993).

2.6. Whole-mount staining

The TM was removed from the gut epithelium and fixed in 4% paraformaldehyde and dehydrated in an ethanol series. The tissue was rehydrated and placed in distilled water. The muscle strips were rinsed for 15 min in PBST and incubated in blocking solution overnight at 4 °C. Incubation for 48–72 h with primary antibodies followed, and the strips were rinsed with the blocking solution for 3 h at 4 °C. Secondary antibodies were applied overnight at 4 °C. The tissue was rinsed with blocking solution (1X PBS/5% normal serum from the same species as the secondary antibody /0.3% Triton™ X-100) overnight at 4 °C and stained with 0.1 μg/ml Hoechst dye for 5 min to visualize nuclei. The entire procedure was performed with agitation. Finally, the TM was rinsed for 15 min in PBST and mounted on microscope slides in glycerol–PBS for visualization.

2.7. Antibody list

Anti-GFP,Mouse, monoclonal (1:100) Millipore [MAB3580, RRID: AB_94936],; Anti-GFP,Rabbit, polyclonal (1:100), Invitrogen [A-11122, RRID: AB_221569]; Anti-nestin,Mouse, monoclonal (1:200), Millipore [MAB353, RRID: AB_94911]; Anti-SOX10, Rabbit, polyclonal (1:150), Millipore [AB5727, RRID:AB_2195375]; Anti-GFAP (glial fibrillary acidic protein), Rabbit, polyclonal(1:400), BTI [BT575]; Anti-peripherin, Rabbit, polyclonal, (1:500), Millipore [AB1530, RRID: AB_90725]; Anti-PDX1, Rabbit, polyclonal (1:50), Cell Signaling; Anti-PDX1 [5679, RRID: AB_10706174], Mouse, monoclonal (1:50), DSHB [F6A11, RRID: AB_1157904], Anti-amylase, Rabbit, polyclonal (1:500), Abcam [ab21156, RRID: AB_446061]; Anti-C-peptide, Rabbit, polyclonal (1:200), Abcam [ab14181, RRID: AB_300968]; Anti-tubulin isotype III (neuron specific βIII-tubulin), Mouse, monoclonal (1:500), Sigma [T8660, RRID:AB_477590]; Anti-MAP2 (microtubule associated protein), Mouse, monoclonal (1:100), Millipore [MAB3418, RRID: AB_94856]; Anti-GFAP (BTI575), Mouse monoclonal (1:200), Sigma [G3893, RRID: AB_477010]; Anti-VIP (vasoactive intestinal peptide), Rabbit, polyclonal (1:100), USBiological [V2115-01, RRID: AB_2216418]; Anti-neuropeptide Y (NYP), Rabbit, polyclonal (1:100), Sigma [N9528, RRID: AB_260814]; Anti-serotonin, Mouse monoclonal (1:200), GeneTex [5-HT-H209, RRID: AB_792022]); Anti- calretinin, Rabbit, polyclonal (1:50), Novus Biologicals [NBP1–32244, RRID: AB_10003923]; Anti-TH (Tyrosine Hydroxylase), Rabbit, polyclonal (1:800), Millipore [AB152, RRID: AB_390204]; Anti-NOS (Nitric Oxide Synthase), Rabbit, polyclonal (1:100), Novus Biologicals [NB100–858, RRID: AB_2236048]; Anti-P75 NGF receptor, Mouse monoclonal(1:150), Abcam [ab3125, RRID: AB_303531]; Anti-NF (Neurofilament), Mouse monoclonal (1:200), Millipore [MAB5266, RRID: AB_2149763]; Anti-S100ß, Mouse monoclonal (1:1000), Sigma [S2532, RRID: AB_477499], Mouse monoclonal Anti-Smooth Muscle Actin, Sigma [A5228, RRID: AB_262054]. Secondary Antibodies (Molecular Probes): AlexaFluor 405 Goat anti-Rabbit [A-31556, RRID: AB_221605], AlexaFluor 405 Goat anti-Mouse [A-31553, RRID: AB_221604], AlexaFluor 488 Goat anti-Rabbit [A-11034, RRID: AB_2576217], AlexaFluor 488 Goat anti-Mouse [A-11001, RRID: AB_2534069], AlexaFluor 568 Goat anti-Rabbit [A-11011, RRID: AB_143157], AlexaFluor 568 Goat anti-Mouse [A-11004] (RRID: AB_141371), AlexaFluor 647 Goat anti-Rabbit [A-21245, RRID: AB_2535813], AlexaFluor 647 Goat anti-Mouse [A-21325, RRID: AB_141693].

2.8. RT-PCR

Total RNA was extracted from single spheres using an RNeasy extraction kit (Qiagen). RNA was quantified using NanoDrop ND-1000 spectrophotometer and converted to cDNA using superscript III (Invitrogen), random hexamer primer (Fermentas) and oligo(dT) primer (Fermentas) in a GeneAmp PCR System 9700 (Applied Biosystems). PCR reactions were performed for 35–40 cycles. Forward and reverse primers (5′-3′) and annealing temperatures were as follows: GAPDH forward 5′-AACTTTGGCATTGTGGAAGG-3′, reverse 5′- ACACATTGGGGGTAGGAACA-3′(annealing temperature, 60 °C), Pdx1 forward 5′- CGACATCTCCCCATACGAAGT-3′(annealing temperature, 56 °C). Reactions included a negative control (no template). Positive control tissue included freshly isolated adult mouse islets (Seaberg et al., 2004; Smukler et al., 2011).

2.9. Microscopic observation and cell quantification

Imaging was performed using a Zeiss LSM510 confocal microscope running software version 3.2 SP2 or an Olympus FluoView1000 confocal system running software version 2.0c and AxioVision v4.6 imaging software (Zeiss).

All quantification of cells was performed using confocal slice images. Images were enhanced using Paint-Shop-Pro software. All changes in the images (merging/separation channels, modifications of contrast, brightness, sharpening) were made evenly across the entire field, and no features were removed or added digitally. All statistical tests were performed using GraphPad Prism version 5.01. Statistical comparisons were performed using analyses of variance (ANOVA) with subsequent Bonferroni post-test tests for comparisons between groups. The number of analyzed experiments (n) was ≥ 3 mice, and data were shown as means ± SEMs, $p < 0.05$.

Time-lapse microscopy: The piece of gastrointestinal tract containing early duodenum and pancreatic bud from Pdx1-Cre x Rosa-YFP E11.5 embryo was placed on a GS Millipore filter secured by silicone grease in a 5 mm culture dish (Corning). The culture dish was filled with DMEM/F12 media (Gibco-BRL) containing 2% B-27 supplement (Gibco-BRL), 100 μg/ml penicillin, 100 μg/ml streptomycin, and 10% fetal calf serum (Gibco-BRL). Media were covered with a layer of mineral oil to prevent evaporation (Fisher Scientific, Pittsburg, PA). The dish was placed on the heated stage of an inverted stage microscope (Zeiss Axiovert 200 M live cell imaging system) and images were taken with AxioCam HRm camera every 1 h. The cells did not show any evidence of phototoxicity, such as membrane blebbing.

3. Results

3.1. The TM of the adult mammalian gut contains a previously unidentified population of multipotent Pdx1-Cre lineage progenitors

Previous studies have shown that NC stem cells persist in the postnatal mammalian gut (Kruger et al., 2002). These multipotent NC precursors were isolated from the muscle layers, but never from the gut epithelium (Kruger et al., 2002). We cultured dissociated cells from the TM of proximal gut of 10 week old CD1 mice (Fig. 1A,B) in defined serum-free media (SFM) (Tropepe et al., 1999) conditions at clonal density (Coles-Takabe et al., 2008). Floating colony formation was observed after 1 week (Fig. 1C). Single cells from dissociated gut tissue itself (separated from the TM) did not form any spheres under the same culture conditions. Although many of the colonies were morphologically similar to brain or NC derived neurospheres (Seaberg and van der Kooy, 2002; Estrada-Mondaca et al., 2007), a clear diversity in size was observed (Fig. 1C). Further lineage tracing experiments (described below) have confirmed the different development origins and fates of the smaller (20–50 μm) versus bigger (50–200 μm diameter spheres (Fig. 1D, Table 1). As expected, generation of cells that express markers commonly produced in gut neural crest derivatives was observed upon differentiation of the larger size (50–200 μm in diameter) colonies in low serum on an adherent substrate (Table 1). These spheres gave rise to cells that expressed SOX10 (the early NC marker found in the embryonic gut (Young et al., 1999)) when put into differentiation conditions (Fig. 1E). Additionally, generation of peripheral neurons and glial cells (both are derivatives of NC stem cells) was observed in differentiated cultures of 50–200 μm spheres (Fig. 1F,G; Table 1). On the other hand, the smaller diameter (20–50 μm) single clonal spheres generated separate cell types that expressed either pancreatic or neuronal markers (Seaberg et al., 2004) under identical differentiation conditions (Fig. 1H-J), whereas bigger diameter spheres did not generate any pancreatic descendants. Indeed, the lineage tracing analyses below revealed that exclusively the small diameter (20–50 μm) spheres arise from the Pdx1 (Pancreatic and Duodenal Homeobox 1)-Cre lineage. It therefore appears that large and small spheres have differing lineage restrictions and potential fates.

3.2. Adult TM-derived Pdx1-Cre lineage progenitor cells are not of NC origin

Pancreas development begins at embryonic day (E) 8.5–9 when Pdx1 - expressing progenitors from the primitive duodenal level epithelium start to give rise to the first pancreatic cells (Guz et al., 1995; Edlund, 1999). At E 9–9.5 migrating NC cells reach the rostral foregut and populate developing pancreatic buds (Young et al., 1998; Young et al., 2003). To ask if multipotent clonal sphere forming progenitors from the TM of the adult gut originated from the Pdx1 (pancreatic) or Wnt1 (neural crest) lineages, we performed lineage-tracing experiments using Pdx1-Cre (Gu et al., 2002) or Wnt1-Cre (Danielian et al., 1998) mice crossed with the Rosa-YFP (Srinivas et al., 2001) reporter strain. This system permanently labels cells that currently are expressing or have expressed the mentioned markers.

Using Pdx1-Cre x Rosa-YFP transgenic mice we observed the formation of YFP expressing smaller diameter spheres (20–50 μm) and YFP-negative bigger diameter spheres (50–200 μm) from the TM of the adult duodenum, ileum and colon (Fig. 2A, Fig. 1D) after 1 week of culture. The frequency of Pdx1-Cre lineage sphere formation was significantly greater in the colon (Fig. 2B), which is the most distant portion of the intestinal tract, than in the duodenum and ileum. YFP+ spheres represented significantly smaller portions of whole sphere population than YFP- within each of these gut segments (Fig. 2B). Surprisingly, this pattern is the opposite of that observed for differentiated Pdx1-Cre lineage neurons, which have their highest frequency in the duodenum (see below). Similar Wnt-1-Cre lineage tracing experiments (to sample the neural crest derivatives) were performed employing Wnt1-Cre x Rosa-YFP adult mice. YFP+ 50–200 μm diameter clonal spheres of Wnt1-Cre lineage were found in the cultures in numbers and proportions similar to YFP negative spheres in the Pdx1 lineage tracing experiments (compare the yellow bars in Fig. 2D to the white bars in Fig. 2B).

The frequency of Wnt1-Cre YFP negative spheres was higher than the frequency of YFP+ spheres from Pdx1-Cre progeny (Fig. 2B,D). There were no Wnt1-Cre lineage positive spheres amongst the smallest (20–50 μm) diameter spheres isolated from Wnt1-Cre x Rosa-YFP adult mice (Fig. 1D). Given the combined findings that no Wnt1 lineage clonal spheres were seen among the smaller spheres and no Pdx1 lineage spheres were seen amongst the larger spheres, it seems that 28% of 20–50 μm and 20% of 50–200 μm diameter spheres may arise from neither of the Pdx1-Cre or Wnt1-Cre lineages, respectively (comparing these non-labeled percentages from the separate Pdx1 and Wnt1 lineage traced mice) (Fig. 1D). These non Pdx1-Cre and non Wnt1-Cre lineage spheres did not generate endoderm or exocrine pancreatic progeny upon differentiation and may represent a different sphere-forming precursor population, possibly mesoderm derived from Myf5 lineage somites (Jinno et al., 2010). The highest frequency of Wnt1-Cre-lineage spheres was observed from the TM of the colon (similar to Pdx1-Cre lineage colonies, see above); and NC clonal sphere

Table 1
Comparison of the mean percentages of neural and pancreatic cell progeny generated from clonal spheres formed from FACS-sorted dissociated TM of Pdx1-Cre x Rosa-YFP mice.

Spheres formed from FACS-sorted dissociated TM of Pdx1-Cre x Rosa-YFP mice	PDX1-positive cells	c-peptide-positive cells	amylase-positive cells	βIII-tubulin-positive cells	GFAP-positive cells
YFP+ spheres	6.2 ± 1%	0.8 ± 0.1%	3.2 ± 0.7%	82 ± 4%	0%
YFP- spheres	0%	0%	0%	86 ± 2.3%	11 ± 1.2%

The number of each cell type is shown as a percentage of Hoechst –positive nuclei. Data represent means % ± SEMs.

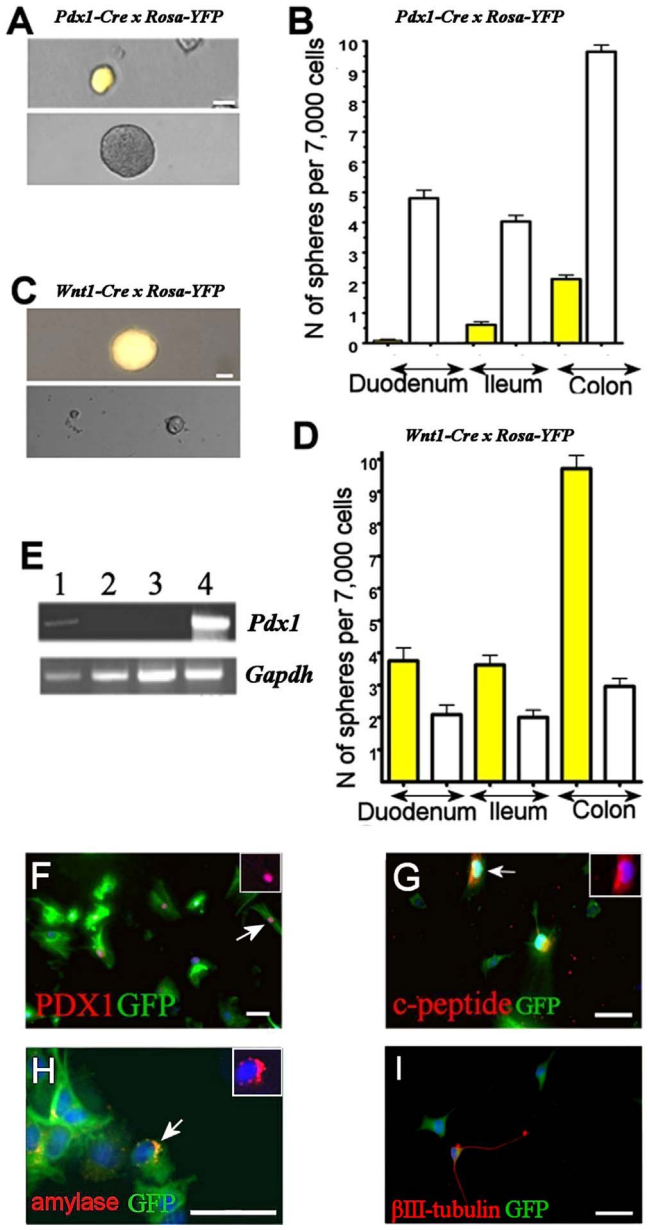

Fig. 2. Lineage tracing identifies the separate Wnt1-Cre and Pdx1-Cre origins of TM-derived sphere-forming cells. (**A**) Small diameter spheres expressing endogenous YFP from the Pdx1-Cre lineage (top) and large diameter YFP- spheres (bottom) from dissociated TM of Pdx1-Cre x Rosa-YFP adult mice. Scale bar for both = 50 μm. (**B**) Frequencies of Pdx1-Cre+ clonal sphere formation (yellow bars) and non Pdx1/Cre clonal sphere formation (white bars) from TM of different anatomical locations within the gut. A two-way ANOVA revealed a significant interaction of gut location and Pdx1 lineage or not ($F_{(2279)}$ = 34.6, $p < 0.0001$. (n = 15 mice dissected with an average of 196 spheres were analyzed per mouse). There were more non Pdx1-Cre lineage spheres (white – YFP-) than Pdx1-Cre lineage (yellow – Pdx1+) spheres, but that both types of spheres were more frequent with more caudal dissections. Bonferroni comparisons showed that both types of spheres were more frequent in the colon that in the duodenum (ps < 0.05). (**C**) Large YFP+ spheres from the Wnt1-Cre lineage (top) and small-size YFP- spheres (bottom) from dissociated TM of adult mice. Scale bar for both = 50 μm. (**D**) YFP+ (yellow bars) and YFP- clonal sphere formation among different anatomical locations within the gut of adult mice. A two-way ANOVA revealed a significant interaction between gut area and Wnt1 lineage or not ($F_{(2138)}$ = 41.8, $p < 0.0001$, n = 17 mice dissected). Bonferroni tests revealed that Wnt1 lineage spheres (yellow – YFP+) and non Wnt1 lineage spheres (white – YFP-) were more frequent with more caudal dissections (ps < 0.05). Data represent means ± SEMs. (**E**) Single sphere RT-PCR analyses of Pdx1 mRNA expression: lane1: YFP+ from Pdx1-Cre x Rosa-YFP TM, lane2: YFP- sphere from Pdx1-Cre x Rosa-YFP TM, lane3: YFP+ sphere from Wnt1-Cre x Rosa-YFP TM, lane4: positive control (RNA from adult islets). (**F-I**)YFP+ spheres generated from FACS sorted adult Pdx1-Cre x Rosa-YFP TM cells give rise to pancreatic progeny (**F-H**) and neuronal progeny (**I**). Insets show separate channel for specific protein staining in the cells indicated by the arrow. Scale bars: (**F-H**) = 20 μm, (**G,I**) = 50 μm.

formation frequencies in the duodenum and ileum did not differ significantly (Fig. 2D). Thus, the colon TM contains the highest frequencies of sphere forming cells from both of the NC and Pdx1- Cre lineages compared to other portions of the gut TM (Fig. 2B,D).

The differentiation of YFP+ spheres from the dissociated and FACS-sorted TM of Pdx1-Cre x Rosa-YFP mice revealed a variety of differentiated pancreatic cell types expressing endoderm, as well as endocrine markers or separate exocrine markers (Fig. 2E,F-H, Table 1). However, the majority, of descendants of Pdx1-Cre lineage spheres were immature neurons (Fig. 2I, Table 1). Clonal spheres derived from YFP negative cells did not give rise to any Pdx1-Cre progeny (Table 1). Intriguingly, no expression of the glial cell marker GFAP, (glial acidic fibrillary protein) by Pdx1-Cre YFP+ differentiated spheres was observed; Pdx1-Cre lineage adult progenitors are capable of generating neurons but not GFAP+ cells under these in vitro conditions. Single genetically marked spheres from each of the Pdx1-Cre and Wnt1-Cre lineages were further tested for the presence of Pdx1 mRNA. This transcript was found only in YFP+ cell (Pdx1-Cre) derived spheres (Fig. 2E).

To compare the capacity of the Wnt1-Cre and Pdx1-Cre -derived spheres for self-renewal, we dissociated genetically labeled clonal colonies into single cells and then plated these cells under the same non-adherent sphere forming culture conditions (at 7000 cells/ml) for 7 days to analyze their ability to form secondary colonies. The majority of single Wnt1-Cre lineage primary spheres gave rise to at least one daughter colony (85 ± 0.9%), whereas only very few (0.5 ± 0.1%) Pdx1-Cre lineage derived single spheres generated secondary colonies, suggesting that these different precursors have different self-renewal and/or survival potentials. Thus, our lineage tracing observations confirm the presence of at least two different types of clonal sphere forming cells in the TM of adult mice (that arise from separate pancreatic and NC origins and that are able to proliferate and form colonies), but that differ in diameter, self-renewal and differentiation potentials.

3.3. The TM of adult mice contains neuronal but not glial endodermal-derived progeny in vivo

To trace the Pdx1-Cre progeny in the adult gut, again the Pdx1-Cre x Rosa-YFP strain of transgenic mice was used. Using confocal microscopy we observed anti-GFP antibody labeled cells (to stain the YFP cells) in the TM of 10 week-old mice mostly between CML and LML within the sites corresponding to the MP (Fig. 3A). Only rare YFP-positive cells were found below the CML in the SP (data not shown). No PDX1 protein expression was found in any portions of intestinal epithelium itself, below the duodenum (data not shown). Pdx1-cre lineage staining also marked intestinal epithelial cells in some villi but not others of the duodenum, suggesting Cre expression in not all gut epithelial stem cells. Immunolabeling with an anti-GFP antibody of adult Wnt1-Cre x Rosa-YFP gut revealed the presence of YFP+ cells within MP and SP plexi (Fig. 3B). Whole mount duodenal TMs from each of Wnt1 and Pdx1 lineage labeled mice were co-stained for the neuronal marker MAP2 and the YFP protein using immunohistochemistry. Double labeled cells, as well as cells only stained for YFP (presumably glial cells or NC stem cells), were found within the Wnt1-Cre x Rosa-YFP MP (Fig. 3C). However, some MAP2+ neurons did not express the YFP protein, suggesting the distinct non-NC origin of these neurons (Fig. 3C,D). Similar analyses of Pdx1-Cre x Rosa-YFP MPs revealed the presence of MAP2/YFP double-positive cells (confirming their Pdx1 origin), as well as MAP2 only and YFP only labeled cells (Fig. 3D-F). In line with our in vitro data, no GFAP/GFP co-staining was observed in the MP of Pdx1-Cre x Rosa-YFP mice (Fig. 3G-J), suggesting a non-Pdx1-Cre lineage origin of all glial cells in the ENS. To confirm this suggestion we examined the Pdx1-Cre x Rosa-CAG-TdTomato 1 week-old mouse gut for the expression of another enteric glia marker, S-100β. No Pdx1-Cre-derived cells were

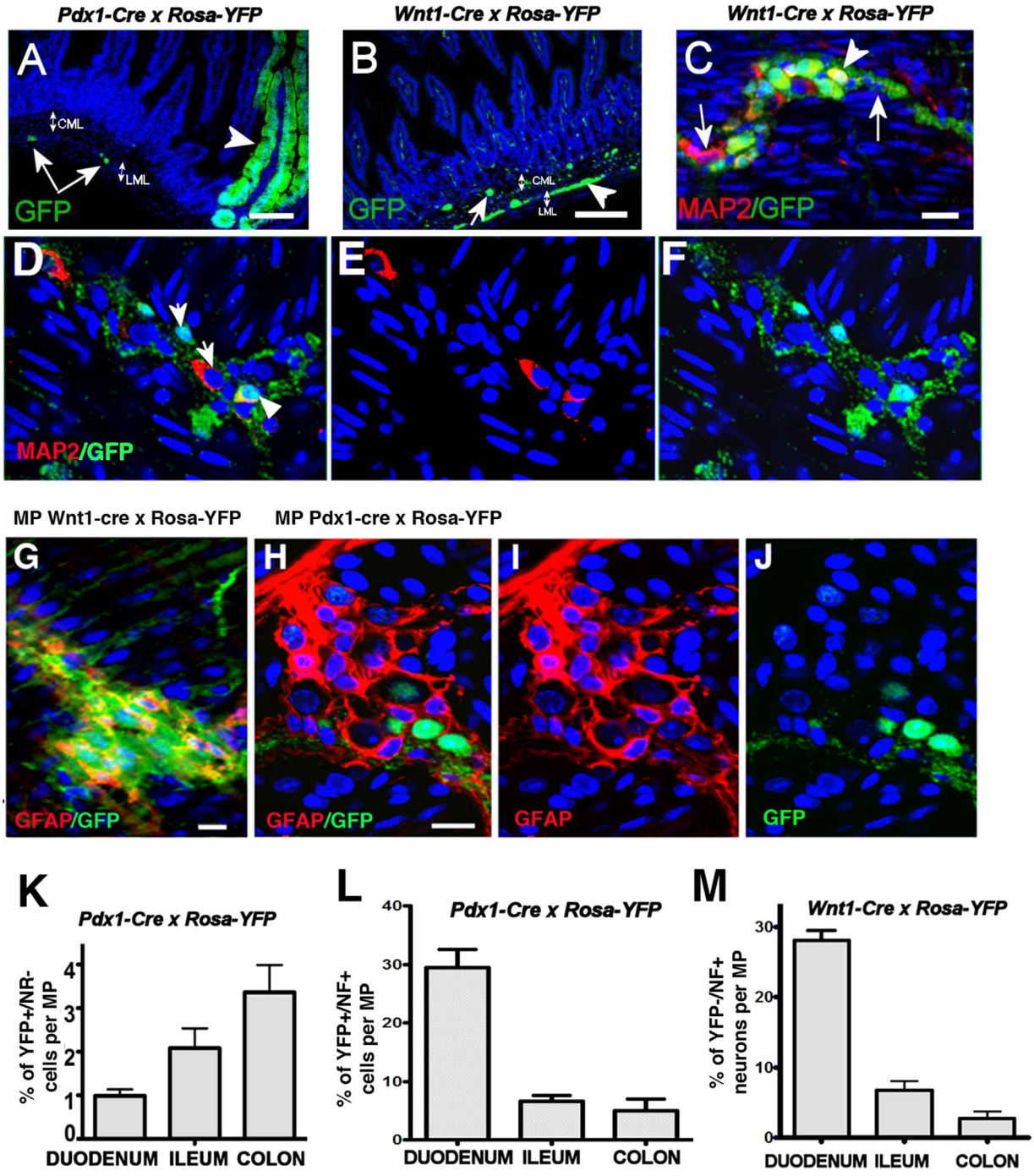

Fig. 3. Neurons of TM layer in Pdx1-Cre x Rosa-YFP adult transgenic gut, but not glia, are Pdx1-Cre progeny. (**A**) Confocal analysis of anti-GFP staining in the TM of adult duodenum/ileum border at the myenteric plexis (MP) level (arrows). Arrowhead points at transgene expression in the duodenal epithelial cells. (**B**) Anti-GFP staining of the duodenum. Arrow: YFP expression at the SP level, arrowhead: at the MP level. (**C**) Whole mount staining of MP: arrowhead indicates the Wnt1-Cre -derived double-positive neuron and, arrows show single-labeled cells. Map2-positive/ YFP-negative neurons (Arrowheads) in the MP of Wnt1-Cre Mice. (**D-F**). Whole mount staining of MP shows the presence of Pdx1-Cre-derived neurons (arrowhead), NC-derived neurons (MAP2+) and Px1-Cre-derived progenitors (YFP+ cells) (arrows). (**G**) Whole mount staining of Wnt1-Cre x Rosa-YFP MP. (**H-J**) Pdx1-Cre x Rosa-YFP MP does not contain Pdx1-Cre-derived GFAP+ glial cells: (**I,J**) there is no overlap between red (GFAP) and green (YFP) channels. Scale bars: (A,B) = 100 μm, (C,G,H,I,J) = 20 μm, (D,E,F)= 10 μm. (**K**) Analysis of the percentage of YFP+/NF- cells in the MP (an one way ANOVA revealed a main effect of location ($F_{(2,11)} = 8.889$, df= 2, $p < 0.01$, n = 26) and multiple comparison tests showed that the colon contains the highest number of non-neuronal cells from Pdx1-Cre progeny, $p < 0.05$). Data represent means ± SEM. (**L**) Analyses of the percentages of Pdx1-Cre-derived neurons in the MP. The absolute number of Pdx1-Cre-derived neurons counted per field of vision is 30.75 ± 4.1 (total 107 ± 3.4) in duodenum, 7.8 ± 0.9 (127 ± 1.6) in ileum and 5.1 ± 1.1 (112 ± 2.1) in colon. A two way ANOVA on the data presented in both L and M revealed only a significant main effect of location in the gut ($F_{(2,8)}= 267$, $p < 0.0001$), with no significant main effect of lineage marker, nor any significant interaction of location in the gut and lineage marker. These results reveal that the numbers of proportion of Wnt1-/NF+ cells in each segment of the gut are the same as the proportion of Pdx1 + /NF+ cells. **M**) Analysis of the percentage of neurons (NF +) from YFP-negative progeny in the MP of Wnt1- Cre mice .

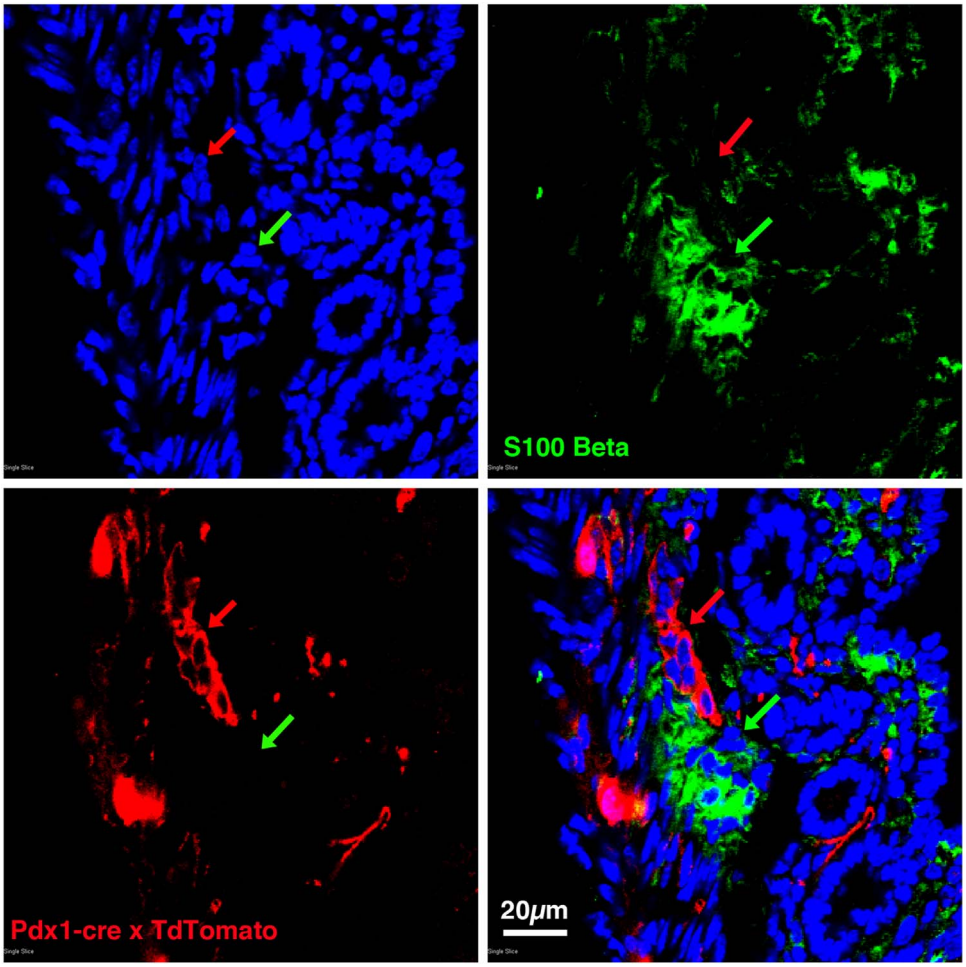

Fig. 4. Duodenal tissue confocal imaging of immunofluorescent costaining with anti-S100ß glial marker antibodies of 1 week old Pdx1-Cre x Rosa-CAGTdTomato mouse. Split channels show no co-expression of lineage (red) and glial marker (green) confirming the non Pdx1 origin of glial cells. Red arrow points to a S100ß-positive cell cluster that doesn't express the lineage marker (GFP, indicated by the green arrow). Cell nuclei were counterstained with Hoechst stain (blue).

found among S-100β positive glial cells (Fig. 4). Indeed, all cells that expressed GFAP were GFP+ in the MP of Wnt1-Cre x Rosa-YFP mice (Fig. 3J). Some non-neuronal, but GFP+, cells residing in the MP of Pdx1-Cre x Rosa-YFP mice may represent Pdx1-Cre-derived multipotent progenitors that are able to form spheres in the in vitro assays.

We compared the numbers of Pdx1-Cre-derived neurons as percentages of all neurons in the MP over the different portions of the mouse intestinal tract (Fig. 3L, Fig. 5A). Pdx1-Cre lineage cells were not seen in the esophagus. In the MP of the adult duodenum, 29.5 ± 5% of neurofilament+ cells also expressed YFP, however the percentages of Pdx1-Cre -derived neurons decreased throughout the length of gut (6.5 ± 1% in the ileum and 5 ± 2% in the colon) (Fig. 3L). The percentages of non-NC-derived neurons in the MP (Wnt1-Cre x Rosa-YFP-) throughout each segment of the gut (Fig. 3M) were not statistically different from the distribution patterns of Pdx1-Cre x RosaYFP+ lineage neurons (Fig. 3L). On the other hand, the percentages of non-neuronal Pdx1-Cre -derived cells within the MP increased significantly from the duodenum to the colon (duodenum- 0.99 ± 0.2%, ileum- 2.04 ± 0.4%, colon- 3.36 ± 0.6%) (Fig. 3K). This pattern (increasing proportions moving from proximal to distal gut) also was seen in the Pdx1-Cre-lineage sphere formation assay (Fig. 2B), suggesting that Pdx1-Cre-derived progenitors reside more in distal portions of the gut, whereas neurons from Pdx1-Cre progeny innervate more prominently the proximal gut. These results provide evidence for the existence of two populations of enteric neurons coming from two different origins: Pdx1-Cre-derived neurons as well as neurons from a different lineage (NC derived neurons; Fig. 3C). The mouse ENS contains at least 11 subtypes of myenteric neurons expressing different markers (Sang and Young, 1996). To determine which classes of neurons develop from endodermal Pdx1-Cre lineage origin, we looked at the expression of the most common neurotransmitters and neuromodulators in YFP+ labeled cells of the MP from Pdx1-Cre x Rosa-YFP mice. Our analyses revealed that YFP-positive and YFP-negative neurons (from both Pdx1-Cre and non- Pdx1-Cre origins, respectively) express VIP, TH, serotonin, NOS, calretinin, and NPY (Fig. 5D-I), and thus and no specific types of neurons could be identified as Pdx1-Cre progeny only. To confirm the presence of neurons labeled by another endoderm marker in the ENS, we analyzed Sox17-2A-iCre (an improved Cre knock-in allele), as an early endoderm lineage tracing strain (Engert et al., 2009). We crossed Sox17-2A-iCre mice with ROSAmT/mG mice, and examined the TM of postnatal day 1 (Engert et al., 2009). The epithelial cells in the gut were labeled by GFP as expected (Fig. 6A-D). Moreover, we observed that GFP-labeled neuronal cells are clustered between the CML and the LML in some (Fig. 6B-D) but not all (Fig. 6F) gut regions when we stained with the early neuronal marker βIII-tubulin. In the MP of duodenum, GFP positive neurons accounted for 35 ± 3% of all neurons, comparable to the percentage of Pdx1 lineage derived neurons using Pdx1-Cre; Rosa-YFP (Figs . 3L and 6E). Most interesting,

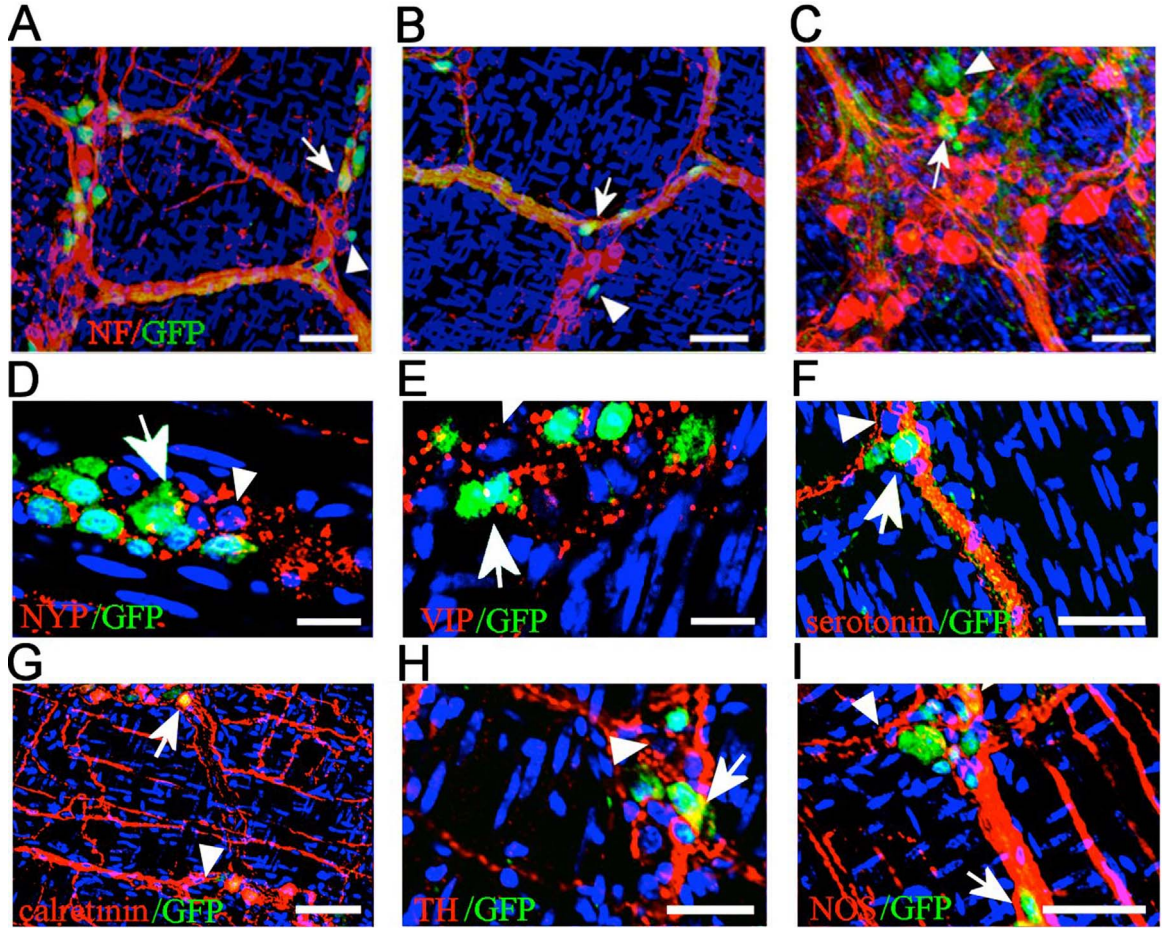

Fig. 5. Whole mount immunofluorescent co-staining of Pdx1-Cre x Rosa-YFP MP derived neurons with subtype markers: (**A**) Duodenum, (**B**) Ileum, (**C**) Colon shows the presence of Pdx1-Cre-derived NF positive neurons (indicated by the arrows, yellow) and non-neuronal GFP-positive cells (arrowhead, green) residing in the myenteric plexuses along the intestinal tract. Cell nuclei were counterstained with Hoechst stain (blue). **(D-I)** Pdx1-Cre-derived neurons express the same types of neurotransmitters and neuromodulators as neural crest-derived neurons. Confocal imaging of whole mount stained MP from Pdx1-Cre x Rosa-YFP adult mouse revealed the expression of NPY (**D**), VIP (**E**), serotonin (**F**), calretinin (**G**), TH (**H**) and NOS (**I**) in neurons from Pdx1-Cre origin (GFP+ cells); arrowheads indicate co-expression of each neurotransmitter with GFP and arrows show GFP- neurons from presumably NC origin expressing similar neurotransmitters as the Pdx1-Cre lineage neurons. Scale bars: **A,B,D,E,F** = 20 μm, **C** = 15 μm, **G** = 50 μm.

the percentage of Sox17-Cre-lineage derived neurons was significantly lower in the ileum and colon compared to the duodenum ($P < 0.01$). This decrease in Sox17 lineage enteric neurons from duodenum to colon is in in line with Pdx1-Cre lineage data, however there still are more Sox17 lineage enteric neurons than Pdx1 lineage enteric neurons in the ileum and colon, perhaps suggesting that some enteric neurons in the intestines originate from more caudal in the endoderm than the duodenum/pancreas. These results show that subsets of myenteric neurons are lineage marked by the Pdx1-Cre and Sox17-1A-iCre transgenes, traditionally considered to mark endodermal lineages

3.4. NC and Pdx1-Cre lineage derived progeny can be distinguished developmentally

Expression from the Pdx1 gene first starts in the mouse posterior foregut endoderm at E8.5 in a region destined to become the antral stomach, pancreas, and rostral duodenum (Guz et al., 1995). We analyzed E10.5 embryos, when YFP labeled Pdx1-progeny cells were detected in the developing duodenal epithelia and forming pancreatic buds (Fig. 7A,B), but not in the sites corresponding to developing ENS (Fig. 7A,B). At this embryonic stage, significant numbers of NC cells had already migrated into the embryonic gut mesenchyme (Druckenbrod and Epstein, 2005) and they expressed the early neuronal marker βIII-tubulin (Fig. 7B). The migration of Pdx1 lineage cells from developing pancreatic tissue and duodenal epithelia starts between E10.5 and E11.5. During this time window, YFP+ cells emerge from the labeled duodenal part of the foregut and from the labeled pancreatic tissue (Fig. 7C-F, Fig. 8A,L, Movie 1). As this separation begins, the cells still co-express Pdx1 protein and the YFP/Pdx1 lineage marker (Fig. 7E,F), however they later lose Pdx1-protein expression (Fig. 8A,B), but remain labeled by the YFP reporter (Figs. 7C and 8A). On the other hand, Pdx1-lineage labeled cells start to express βIII-tubulin when they reach the site of developing ENS at E11.5 (Fig. 7C). Nevertheless, there is no YFP expression in a distal gut portion of E11.5 Pdx1-Cre x Rosa-YFP embryos, whereas at the same stage Wnt1-Cre x Rosa-YFP embryos display robust YFP labeling along the gut tube (Fig. 8B,C), confirming the later migration of Pdx1-Cre enteric progenitors compared to the Wnt1-Cre enteric progenitors. There are no Pdx1-Cre lineage derived enteric progenitors before E11.5 in the developing ENS itself (Fig. 7A,B). To exclude the possibility that some gut NC derived cells express Pdx1 at E11.5, we analyzed Pdx1 protein expression in Wnt1-Cre x Rosa-YFP embryos. No Pdx1 protein+ cells were found among the population of YFP-labeled cells as they migrated past the duodenal/pancreatic area and settled into the ENS site at E11.5 (Fig. 7G,H). At this time point, Wnt1-Cre lineage YFP expression is restricted to the NC derivatives (Fig. 7G), and Pdx1

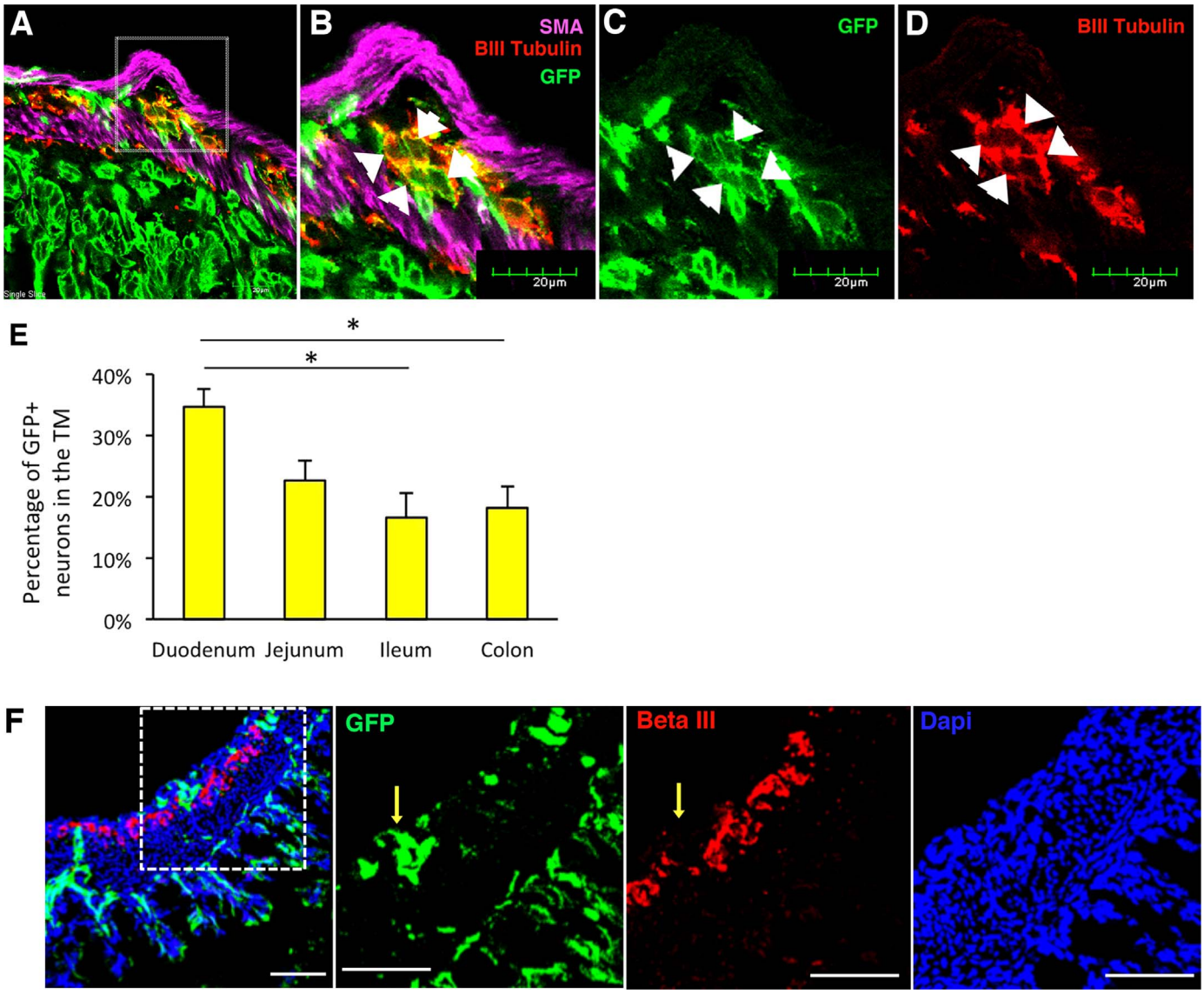

Fig. 6. Lineage tracing with Sox17-Cre x Rosa-mT/mG strain confirms endodermal origin of a subset of ENS neurons. (**A**) Confocal merged image of P1 duodenal oblique sagittal section (partway between a cross section and a longitudinal section) stained with anti- GFP, (AlexaFluro488, Green), Smooth Muscle Actin (SMA) (AlexaFluor405, Purple) and βIII-tubulin (AlexaFluor647, Red) [TdTomato channel not shown]. The green only cells at the bottom of the lineage are Sox17 lineage duodenal epithelial cells. (**B-D**) split images from magnified framed region: arrows point on YFP expression in the Sox17-Cre-derived epithelial cells that also express neuronal marker βIII-tubulin. Scale bar = 20 µm (**E**) Quantification analysis of the percentage Sox17-Cre-derived neuronal cells in the MP of Sox17-Cre x Rosa-mT/mG P1 mice. One-way ANOVA revealed a main effect of location, correlating with Pdx1-Cre lineage tracing data (stars = $p < 0.01$, Bonferroni post hoc tests, n = 18). (**F**) Gut sections from Sox-17-Cre x Rosa-mTmG at Postnatal day 1. Yellow arrows in magnified framed region show that GFP staining (markers of GFP proteins) does not overlap with ßIII-tubulin staining (neuronal marker). Scale bar: 50 µm.

protein is expressed exclusively by duodenal and pancreatic epithelia cells (Fig. 7G,H). Further, the only Pdx1 + /GFP- delaminating cells at this time were seen at the edges of duodenal epithelia (Fig. 8H) whereas GFP+ NC-derived cells surrounded the developing pancreas (Fig. 7G inset**)**. By E13.5 Pdx1-Cre lineage progenitors have migrated along the developing gut tube in a proximal to distal gradient, and contribute to the development of ENS (Figs. 8H-K and 9A). We found that 26% of ßIII-tubulin labeled cells in duodenum are labeled with YFP, and 14% of βIII-tubulin labeled cells in ileum are labeled with YFP. Analyzing E13.5 Sox-17-Cre x mTmG we have found that these percentages were 2.42% ± 0.45% and 1.8% ± 0.25, respectively. Intriguingly, at P1 the number of labeled cells increases to over 20% of MP neurons (Fig. 6E). Such a delay between the onset of Cre transcription and its biological effect has been described by different authors (Li et al., 2008; Nagy, 2000) and can explain the difference of genetically labeled neuron numbers at different stages. It has been shown previously that the Cre in the strain Sox17-iA2-Cre, is expressed in blood vessels (Engert et al., 2009). However, there was no co-localization of the transgene marker and CD 31 (an endothelial marker) observed in sites corresponding to developing ENS (Fig. 9B).

Supplementary material related to this article can be found online at doi:10.1016/j.ydbio.2018.11.014.

To test for the possibility of ectopic transgene expression, we have examined reporter expression in various NC derivatives at E13.5 (Fig. 9). In Pdx1-Cre x Rosa-YFP E13.5 embryos, YFP labeled cells were scattered in spinal cord (Fig. 9C), but were not spotted in DRGs (n = 6 mice). In Sox-17-Cre x mTmG mice, GFP (here GFP is mTmG) labeled cells in the DRGs overlapped with CD31 labeled cells, which is

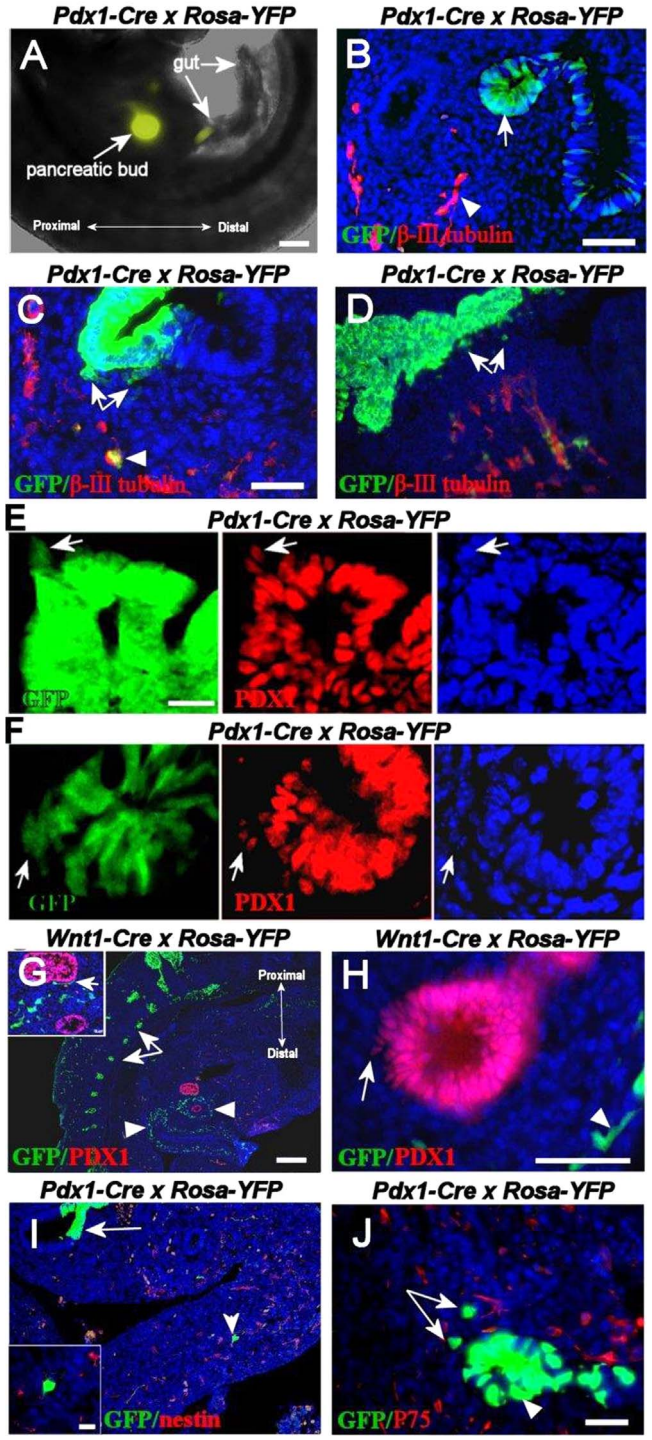

Fig. 7. Migration of ENS Pdx1-Cre-derived progenitors from duodenal and pancreatic epithelia starts at E11.5. (**A-B**) E10.5 embryo. No endogenous YFP presents in the developing TM of the gut (**A**). (**B**) ßIII-tubulin+/YFP- early developing neurons (presumably NC-derived, arrowhead) approaching YFP+ epithelial cells of the foregut (arrow). (**C**) E11.5: YFP+ cells (arrow) emerge from the foregut epithelium toward the site of developing ENS (βIII-tubulin+ cells). Some of them co-express both markers (arrowhead). (**D**) E11.5 embryo: Pdx1-Cre lineage cells (arrows) emerge from the GFP+ pancreata. (**E,F**)) Confocal imaging of the E11.5 pancreatic (**E**) and duodenal (**F**) epithelia reveals PDX1 protein expression in emerging Pdx1-Cre lineage labeled cells (arrows). (**G**) E11.5 Wnt1-Cre x Rosa-YFP embryo displays YFP+ DRGs (arrows) and enteric NC precursors (arrowheads), whereas the developing pancreas specifically express PDX1 protein (inset, arrow points on NC-derived cell attaching pancreata). (**H**) Cells from Wnt1-Cre origin surround the PDX1+ developing gut epithelium (arrowhead) in Wnt1-Cre x Rosa-YFP embryo PDX1+ delaminating cells are observed at the edges of developing duodenum (arrow). (**I,J**) E12.5 embryo: YFP+ migrating cells from Pdx1-Cre origin (indicated by the arrowhead (**I**) and arrow (**J**) do not express Nestin and P75. The YFP+ duodenal epithelium is indicated with an arrow in (**I**) and arrowhead in (**J**). Inset in (**I**) shows a higher magnification of the YFP+/nestin- migrating cell. Scale bars: (**A,G**) = 200 μm, (**B,D**) = 50 μm, (**C,H,J,G,**(inset)) = 20 μm, (**E-F** = 15 μm, (**I**) = 50 μm.

consistent with the Cre expression in blood vessel endothelial cells. In the superior and inferior vagal ganglion of Pdx1-Cre x Rosa-YFP embryos, there were no Pdx1 lineage cells observed (n = 3), however in the superior cervical sympathetic ganglion there were scattered GFP labeled neurons (with an average of 1.73+/- 0.4% of ßIII-tubulin positive cells double labeled with GFP) (n = 5). In the same ganglia of Sox-17-Cre x mTmG, the Sox17 lineage labeled cells were clearly of blood vessel cell shape, and were not labeled by ßIII-tubulin (n = 4) (Fig. 9D). We also looked at the Pdx1 lineage labeling in the E8.5 embryos before the neural crest migrates away from the brainstem and spinal cord. In these Pdx1-Cre x Rosa-YFP embryos (Fig. 10A), there was no YFP+ labeling in vagal neural crest region (consistent with the lack of Pdx1 lineage cells in the vagal ganglia at later ages – Fig. 9G), but some YFP+ cells were scattered in the cervical sympathetic neural crest region (Fig. 10B), consistent with the finding of a small number of Pdx1 lineage neurons in the superior cervical ganglia at later ages (Fig. 9F). Nevertheless, the small numbers of Pdx1 lineage cells in the cervical sympathetic neural crest region at E8.5 (n = 6 per embryo; Fig. 10 caption) and the small numbers of post-mitotic Pdx1 lineage neurons in the superior cervical ganglion (< 2% of neurons) seem unlikely to account for the large numbers of Pdx1 lineage enteric neurons (> 20% of duodenal enteric neurons).

In contrast to NC-derived precursors (Young et al., 1998, 1999; Mujtaba et al., 1998; Lei and Howard, 2011) (Fig. 8D-G), Pdx1-Cre-derived progenitors did not express the NC marker P75 or the common neural precursor marker nestin during embryonic gut colonization at E12.5 (Fig. 7I,J), again confirming their distinct origin. Interestingly, when we crossed another slightly later in development pancreatic lineage tracing line Ptf1a-Cre with Rosa-CAG-TdTomato reporter mice (Ptf1a-Cre x TdRed) to trace the pancreatic precursors, we did not find TomatoRed positive neurons in mice at E15.5; Fig. 10C), while we observed a developing neuronal network labeled by TomatoRed positive neurons in E15.5 Pdx1-Cre x TdRed mice (Fig. 10D).

3.5. Pdx1-Cre reporter labeling reflects endogenous Pdx1 expression

Some recent reports have demonstrated the expression of Cre-recombinase driven reporters by pancreas-specific Pdx1 promoters in the mouse developing brain and inner ear, in the absence of endogenous Pdx1 protein expression, and interpreted this as transgene leakage or nonspecific ectopic expression (Song et al., 2010; Honig et al., 2010; Wicksteed et al., 2010). We also observed an activation of the YFP reporter in the same regions, however Pdx1 protein expression also was detected in E12.5 developing inner ear, but not in the brain (Fig. 11). Six important control experiments excluded the possibility of ectopic Pdx1-Cre transgenic expression in the ENS. First, our Pdx1-Cre results were confirmed by analyzing another endoderm Sox17-Cre knock-in strain (Fig. 6). Second, we have examined a second Pdx1-Cre mouse strain that was developed by insertion of a different transgene into a different genetic locus (Gannon et al., 2000). Although the recombination efficiency (approximately 30% of pancreatic cells) with this Pdx1-Cre line was much less than the first line used, some clonal YFP expressing spheres were generated from the dissociated TM of this second line (Fig. 12A), and expression of the YFP reporter also was observed in some enteric neurons (10% at most) of this second Pdx1-Cre strain (Fig. 12B-D). The total percentages of Pdx1-Cre – derived neurons corresponded to the previously analyzed Pdx1-Cre strain, given the lower recombination efficiency of the second line (Fig. 12G). Third, to confirm partial endodermal origin of the enteric neural system we analyzed E12.5 embryos generated by crossing $Foxa2^{tm2.1(cre/Esr1)Moon/J}$ with Rosa-YFP reporter. Foxa2 is a Forkhead transcription factor required for definitive endoderm formation (Ang and Rossant, 1994). Tamoxifen administration ~E7.5 and ~E9.5 led to YFP labeling of approximately 40% cells in endoderm derivatives in E12 embryos (Fig. 12E), including partial labeling of the developing ENS (Fig. 12E,F). Fourth, no overlap was seen between

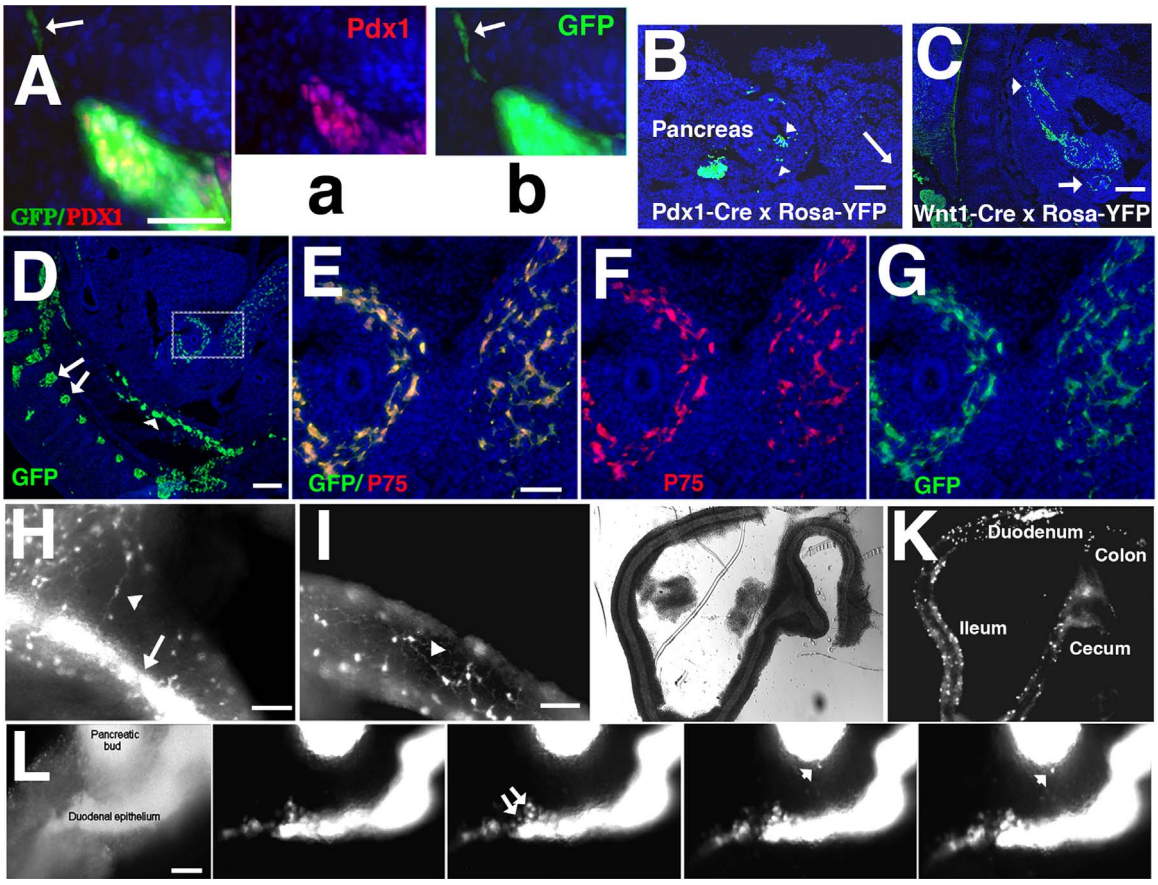

Fig. 8. PDX1-positive cells of the early foregut epithelia lose PDX1-protein expression upon further migration towards ENS sites, but remain labeled by the YFP reporter. (A) PDX1/GFP protein staining of early duodenum shows specific PDX1 (a) and GFP (b) co-expression in the epithelia and only GFP expression in the migrating cells (the enlarged area of A indicated by the arrow). (B,C) Pdx1-Cre x Rosa-YFP progenitors migrate at E11.5, whereas the Wnt1-Cre x Rosa-YFP-derived cell wave already has colonised distal gut mesodermal compartments by this time (B) GFP protein staining of E11.5 Pdx1-Cre x Rosa-YFP embryo shows the reporter presence in the proximal gut (arrowhead) and no YFP staining in the distal portion (arrow). (C) The same E11.5 stage Wnt1-Cre x Rosa-YFP embryo: massive YFP staining around proximal (arrowhead) and distal gut (arrow) is depicted. (D-G) Specificity of genetic reporter labeling in E12.5 Wnt1-Cre x Rosa-YFP embryo ENS. (D) Specific reporter expression in NC derivatives: DRGs (arrows), sympathetic chain cells (arrowhead) and migrating enteric precursors (boxed area). (E-G) P75 and GFP co-labeling of the boxed area: all GFP+ cells express NC marker P75 (F,G). (H-K) Endogenous YFP expression in the digestive system of E13.5 day Pdx1-Cre x Rosa-YFP embryo. Endogenous YFP expression is seen in the future duodenal epithelia (arrow) (H), but is not seen yet in the ileal epithelia (I). Neuron-like morphology cells are present in the gut muscle layer at this developmental stage (H,I arrowheads). (J) Bright field and complementary fluorescent (K) images of developing gut tube show the appearance of Pdx1-Cre-derived (presumably migrating) cells: (K) The most distal gut part (colon) contains fewer fluorescent neurons then proximal gut portions. Scale bars: A,EG = 20 μm, H= 50 μm, B-D, I-K = 100 μm. L. Still photos from live imaging of a Pdx1-Cre x Rosa-YFP E11.5 embryo proximal gut explant: Emerging of Pdx1-Cre-derived progenitors from duodenal epithelium and pancreatic bud. The individual cells expressing an endogenous reporter emerge from YFP+ duodenal epithelia (arrows) and pancreatic bud (arrowheads). Images were taken every 1 h. Scale bar = 50 μm.

Wnt1-Cre; Rosa-YFP+ cells labeled cells and Pdx1 protein expression at E11.5 when NC cells were migrating past the pancreas/duodenum (Fig. 7G,H), whereas complete overlap of Pdx1 protein expression and the endogenous reporter was detected in Pdx1-Cre transgenic line at this same age (Fig. 7E,F). Fifth, little Pdx1-Cre and no Sox-17 transgene expression was found in neurons in various rostral autonomic and DRG ganglia in E13.5 transgenic embryos (Fig. 9C,D), confirming that if there is non-specific Pdx1 transgene expression, it affects only a very small subset of NC-derived cells. Sixth, two types of neural progenitor cells were identified in developing ENS previously: nestin expressing cells that give rise to both neurons and glia and a nestin-negative population that generates only neurons (Lei and Howard, 2011). Pdx1-Cre lineage progenitors were found here to generate only neurons in the ENS and to express neither nestin nor the neural crest marker P75 during embryogenesis (Fig. 7I,J), supporting the existence of a separate, non-neural crest-derived lineage of portions of the ENS.

Intriguingly, analysis of one more pancreatic knock-in lineage tracing line (Ptf1a-Cre) did not reveal the existence of Ptf1a-Cre-derived neurons in the E15.5 embryo (Fig. 10B). It is possible that the endoderm-derived enteric neurons are primarily derived from the duodenum. However, given that the Ptf1a gene is expressed about 1 day later than Pdx1 and is restricted in the pancreatic buds (Kawaguchi et al., 2002), we suggest that it is more likely that the enteric neurons coming from the pancreas may have migrated out of the pancreas before the Ptf1a transgene reporter is turned on in the pancreatic buds (Fig. 12H)

4. Discussion

The present results provide strong evidence for the existence of two embryonic sources for the ENS based on Cre-LoxP transgenic animal models. Previous data suggested that the NC was the sole origin for the ENS, although additional suggestions that the NC also gave rise to cells in the pancreatic endocrine endoderm were not supported by later transplant and lineage tracing experiments (Fontaine and Le Douarin, 1977; Andrew et al., 1983; Jonsson et al., 1994). Here we show the opposite result: the pancreatic/duodenal endoderm (traced with Pdx1, Sox17 and Foxa2 lineage reporters) gives rise to a portion of the neurons in the ENS, particularly in the MP of the proximal gut. Although, we conducted seven control experiments supporting the claim that it is very unlikely that ectopic expression of all of the transgenes employed could explain the present results, it may be

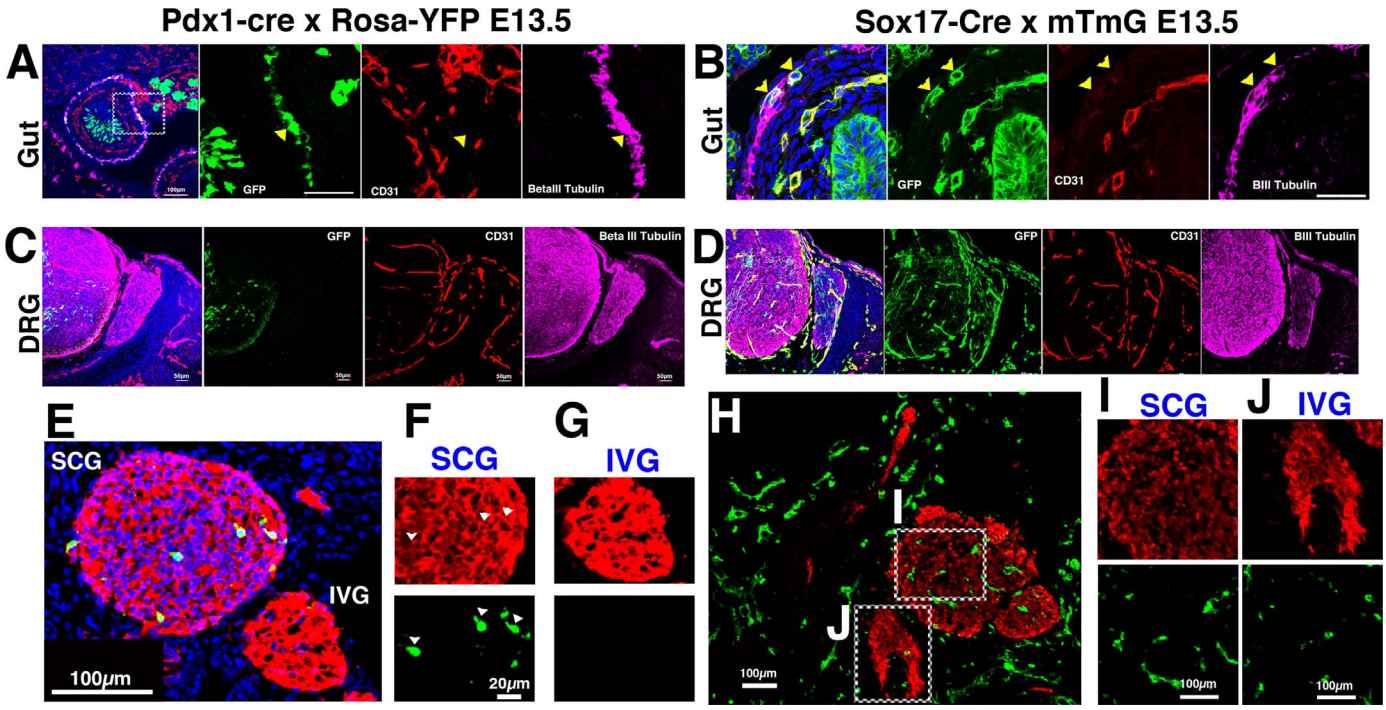

Fig. 9. Lineage tracing in Pdx1-Cre x Rosa-YFP and Sox-17-Cre x mTmG at E13.5. (A) and **(B)** Gut sections of Pdx1-Cre x Rosa-YFP and Sox-17-Cre x mTmG mice, respectively: arrows show overlap between GFP staining and ßIII-tubulin staining (neuronal marker) but not between GFP and CD31. **(C)** There is no transgene expression in E13.5 Pdx1-Cre x Rosa-YFP cervical DRG. **(D)** In Sox-17-Cre x mTmG DRG the transgene is co-stained with an endothelial marker, but not with ßIII-tubulin. **(E)** Very rare transgenic GFP stained cells are seen in the sympathetic superior cervical ganglion, but not in the vagal ganglia of Pdx1-Cre x Rosa-YFP mice. **(F)** A higher magnification picture of the superior cervical ganglion (SCG) shows a few Pdx1 lineage neurons (double labeled with a ßIII-tubulin antibody). **(G)** A higher magnification picture of the inferior vagal (nodose) ganglion shows that no Pdx1 lineage labeled cells. (H). The superior cervical ganglion and vagal ganglia of Sox-17-Cre x mTmG mice show no neuronal labeling of the transgene stained cells **(I)** shows a higher magnification picture of the superior cervical ganglion, and **(J)** shows a higher magnification of the inferior vagal ganglion. Scale bars = 50 μm.

impossible to completely rule out the idea that a small subset of cells does display ectopic transgene expression.

A complete absence of enteric neurons from the proximal intestine of animals homozygous for mutations in NC-specific genes like Foxd3 (Teng et al., 2008) and Sox10 (Herbarth et al., 1998) has been shown previously, supporting the generally accepted idea of an exclusively NC origin of the mammalian ENS. Unfortunately, there is no single and unique marker that is specific for NC identity. Thus, Foxd3, Sox10 and Sox9 (suggested NC markers) are expressed in the developing mouse pancreas (Lioubinski et al., 2003; Perera et al., 2006), and both adult Wnt1-Cre and Pdx1-Cre lineage progenitors were found expressing Sox10 protein in vitro (data not shown). Therefore, Foxd3 and Sox10 mutations may affect Pdx1-Cre lineage progenitors as well as NC cells and mutations in these genes may result in neuronal loss from both sources. Similarly, surgical removal of the vagal neural crest in chick was reported to result in complete loss of neural crest (Yntema and Hammond, 1954), but more recent lineage tracing data in rodents suggests that enteric neurons also arrive from the sympathetic cervical neural crest (Espinosa-Medina et al., 2017). These data along with the present findings suggest multiple origins for enteric neurons.

Further evidence in favour of the two separate lineages hypothesis for the ENS was the persistence of two types of progenitor cells in the TM of the adult mammalian gut. Gut NC stem cells have been described (Kruger et al., 2002; Estrada-Mondaca et al., 2007); however the present report also identifies separate multipotent Pdx1-Cre progenitors within similar gut sites. Pdx1-Cre -derived progenitors in the gut differ from NC stem cells in the gut by an apparently more limited self-renewal capacity, by generating smaller size clonal colonies and by their differentiation potential. The existence of Pdx1-Cre-derived progenitors from pancreatic tissue with the ability to generate both neuronal and pancreatic lineages in vivo and in vitro has been reported previously (Seaberg et al., 2004; Smukler et al., 2011). Separate Pdx1-Cre-derived progenitors and Wnt1-Cre- derived progenitors also are present within the pancreas itself (Arntfield and van der Kooy, 2013). While both extra-pancreatic and intra-pancreatic Pdx1-Cre-derived multipotent cells are labeled by the same genetic marker, they differ remarkably in terms of their development potential. Thus, the pancreas-derived precursors more prominently generated differentiated pancreatic endocrine and exocrine cells (Seaberg et al., 2004) than the Pdx1-Cre lineage gut-derived precursors described here. On the other hand, the Pdx1-Cre lineage adult gut-derived precursors were found to generate more neurons in vitro (from the differentiation of clonal sphere colonies) than did the Pdx1-Cre lineage adult pancreas derived precursors. It is possible that the Pdx1-Cre lineage precursors in the adult pancreas versus gut are intrinsically biased in their differentiation potentials in the early embryo, but it also is possible that are Pdx1-Cre lineage precursors are identical and that the environment that they find themselves in determines their differentiation potentials.

The topographic distributions throughout the gut length of the precursor cells from both Pdx1-Cre and Wnt1-Cre lineages are similar: the greatest proportion of sphere forming cells was isolated from the distal gut, whereas the proximal gut contained fewer precursor cells. However, the distribution of Pdx1-Cre-lineage neurons through the gut tube showed the opposite pattern. Neural progenitors have a more extensive migration potential than differentiated neurons (Babona-Pilipos et al., 2011). We suggest that Pdx1-Cre-derived precursors migrate extensively along the gut tube during embryogenesis, whereas Pdx1-Cre-derived neurons tend to differentiate soon on their arrival in the gut TM. Another possibility is that a more extensive migration of

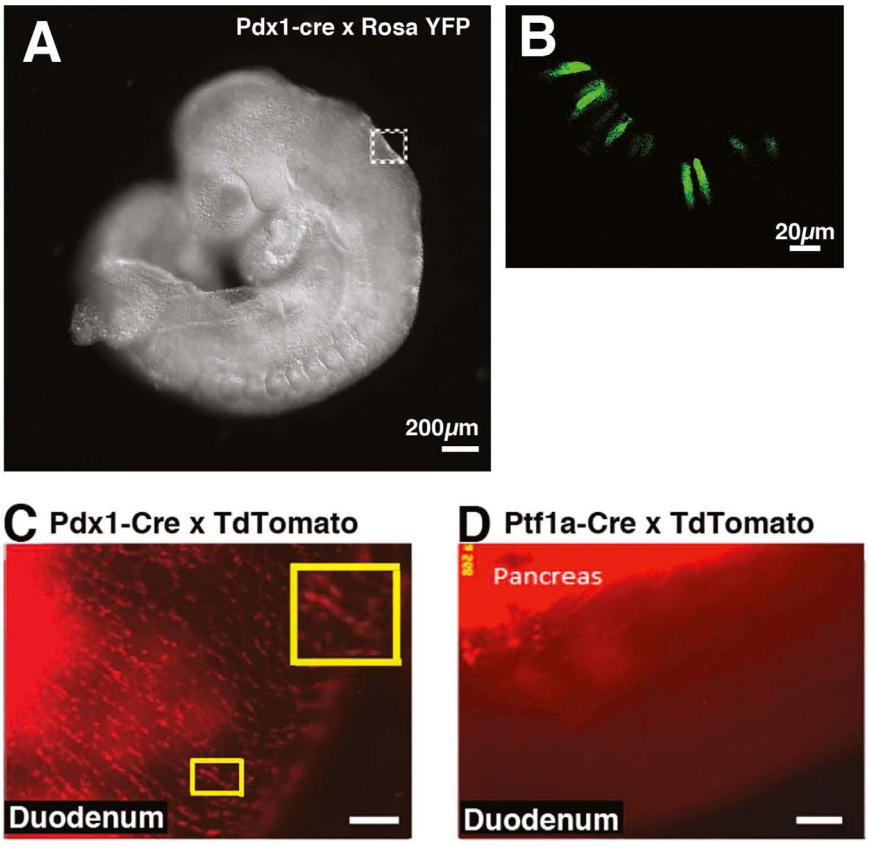

Fig. 10. Lineage tracing of Pdx1-Cre x Rosa-YFP at E8.5. (**A)** Low magnification of the whole embryo at E8.5, with the boxed area showing the location of the inset. (**B)** Inset shows a higher magnification of the area where scattered YFP+ cells are located in the dorsal cervical spinal cord, where neural crest cells delaminate from. Number of YFP-positive cells in the head region = 6 + /- 0.67 averaged across 7 embryos. Scale bars as indicated in the panels. **(C,D)** E15.5 whole mount TdTomato labeling. Both pancreas and gut neuronal networks are labeled by the lineage reporter in Pdx1-cre x TdTomato embryos, whereas in the Ptf1a-Cre x TdTomato embryo only pancreatic tissue is labeled. Inset in **(C)** shows a higher magnification of neurons in the boxed area.

Pdx1-Cre-derived neurons (and gut colonization at E11.5) may be inhibited by pre-existing NC –derived early neurons in these compartments (Hotta et al., 2010). Additional studies will be needed to show definitively the details of migration and survival of Pdx1-Cre derived neurons from the pancreas and duodenum to the enteric nervous system.

Our findings also may shed new light on the etiology of Hirschsprung's disease (HSCR), which is thought to result from NC-related mutations (Amiel and Lyonnet, 2011). HSCR is characterised by the absence of ENS ganglion cells, and functionally this results in an obstruction of the aganglionic gut. The classic form of HSCR is restricted to distal bowel region and only occasionally involves small intestine (Hirschsprung, 1888; Heuckeroth, 2018). It remains to be investigated whether Pdx1-Cre-derived neuronal progenitors might compensate for affected neural crest derived neurons in the more proximal portion of the gut. Alternatively, the lack of NC-derived neurons might affect the survival and migration of Pdx1-Cre-derived precursors.

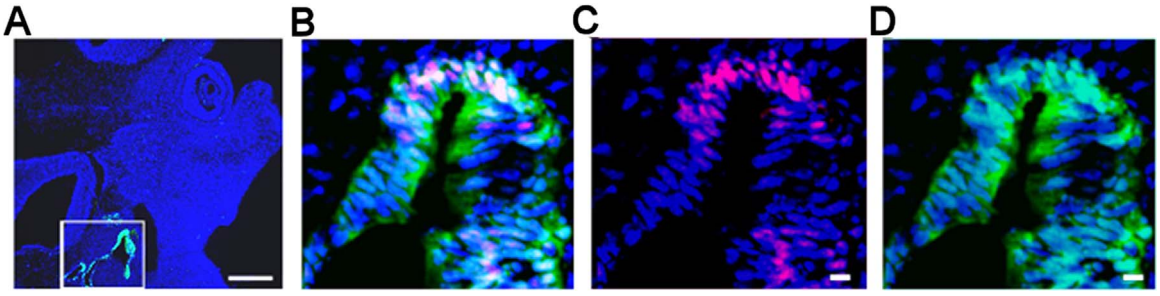

Fig. 11. YFP-reporter expression in the E12.5 Pdx1-Cre x Rosa-YFP embryonic inner ear. (A) Immunofluorescent staining with an anti-GFP antibody of the E12.5 Pdx1-Cre x Rosa-YFP embryonic head shows reporter expression in the inner ear (marked area in **A**). **(B)** Confocal magnified merged image of the marked area stained with anti-GFP and anti- PDX1 antibodies shows the present of PDX1protein positive cells in the some of the GFP labeled cells. **(C,D)** Split channels show specific PDX1 **(C)** and GFP **(D)** expression in the same cells. Cell nuclei were counterstained with Hoechst stain (blue). Scale bars: **A** = 200 μm, **B,D** = 20 μm.

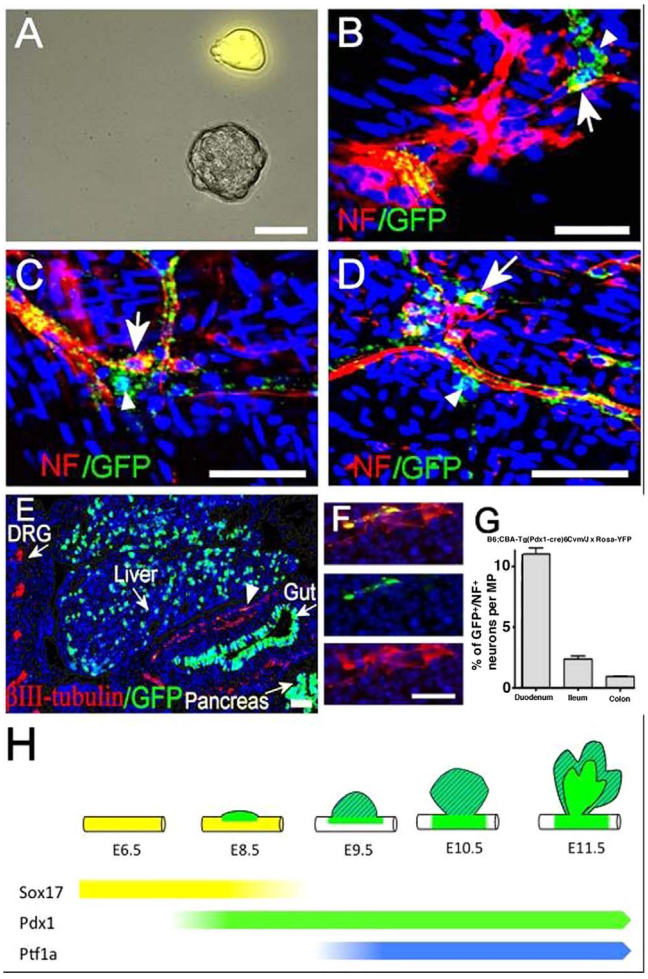

Fig. 12. Analyses of YFP-reporter expression in the B6;CBATg(Pdx1-cre)6Cvw/J x Rosa-YFP strain. (A) A small size YFP+ sphere from the Pdx1-Cre lineage and a larger non-YFP labeled sphere (presumably from a neural crest stem cell) were formed from dissociated gut TM. **(B-D)** Confocal imaging of NF and GFP whole mount adult MP staining: B-Duodenum, C-Ileum, D-Colon. Double positive neurons are indicated by arrows, cells expressing YFP only are indicated by arrowheads. **(E,F)** Analysis of tamoxifen-induced, Cre-mediated endoderm targeted lineage tracing in Foxa2$^{tm2.1(cre/Esr1)Moon/J}$ x Rosa-YFP E12 embryos. Endoderm-derived organs are indicated by the arrows. **(E)** Red βIII-tubulin+ cells surround the GFP+ developing gut. Some of them co-express both markers (one is marked by an arrowhead). **(F)** magnified arrowhead indicated area from **(E)** shows co-localization of GFP and expression of the early neuronal marker βIII-tubulin. **(G)**. Comparative analyses of the percentages of Pdx1-Cre-derived neurons throughout B6;CBA-Tg(Pdx1-cre)6Cvw/J x Rosa-YFP TM, n = 25. Data represent means +/- SEMs. Scale bars: **(A,E,F)** = 50 μm, **(B,C,D)** = 20 μm **(H)** Schematic representations of the embryonic times of expression of different genes in the mouse gut tube and developing pancreas. Sox17 gene is expressed from E6.5 to E8.5in the visceral endoderm and forming definitive endoderm. Pdx1 gene is expressed from E8.5 in the developing pancreatic buds as well as in some of the duodenal epithelial cells. Pdtf1a gene is expressed around E9.5 but restricted to the pancreatic buds.

Acknowledgements

This work was supported by CIHR (CIHR:FDN-14807), the Canada First Research Excellence Fund, and the Juvenile Diabetes Research Foundation Canada, (JDRF:3-SRA-2016-251-S-B). I.B. was supported by a CIHR Training Grant in Biological Therapeutics and a BBDC fellowship J.X was supported by a BBDC (Banting and Best Diabetes Centre) fellowship in Diabetes Care funded by Eli Lilly and Boehringer Ingelheim. We thank for Brian De Veale and Ryan Ting-A-Kee for helpful discussions, Pier-Andree Pentilla for expert assistance with FACS analysis, D. Melton and A. McMahon for generously providing transgenic mice, and Rachel Leeder, Ahmed Fahmy, Samantha Yammine for technical support.

Competing interests

No competing interests declared.

CRediT authorship contribution statement

Irina Brokhman: Conceptualization, Data Curation, Methodology, Writing - original draft, **Jie Xu:** Data Curation, Methodology, Writing - original draft, Writing - review & editing, **Brenda L.K. Coles:** Data Curation, Writing - review & editing, **Rozita Razavi:** Data Curation, **Silvia Engert:** Resources, **Heiko Lickert:** Resources, **Robert Babona-Pilipos:** Data Curation, **Cindi M. Morshead:** Resources, **Eric Sibley:** Resources, **Chin Chen:** Resources, **Derek van der Kooy:** Conceptualization, Methodology, Funding Acquisition, Resources, Writing - original draft, Writing - review & editing

References

Amiel, J., Lyonnet, S., 2011. Hirschsprung disease, associated syndromes, and genetics: a review. J. Med. Genet 38, 729–739.
Andrew, A., Kramer, B., Rawdon, B.B., 1983. Gut and pancreatic amine precursor uptake and decarboxylation cells are not NC derivatives. Gastroenterology 84, 429–431.
Andrew, A., Kramer, B., Rawdon, B.B., 1998. The origin of gut and pancreatic neuroendocrine (APUD) cells–the last word? J. Pathol. 186, 117–118.
Ang, S.L., Rossant, J., 1994. HNF-3 beta is essential for node and notochord formation in mouse development. Cell 78, 561–574.
Arntfield, M., van der Kooy, D., 2011. beta-Cell evolution: how the pancreas borrowed from the brain: the shared toolbox of genes expressed by neural and pancreatic endocrine cells may reflect their evolutionary relationship. Bioessays 33, 582–587.
Arntfield, M., van der Kooy, D., 2013. The adult mammalian pancreas contains separate precursors of pancreatic and neural crest developmental origins. Stem Cells Dev. 22, 2145–2157.
Babona-Pilipos, R., Droujinine, I.A., Popovic, M.R., Morshead, C.M., 2011. Adult subependymal neural precursors, but not differentiated cells, undergo rapid cathodal migration in the presence of direct current electric fields. PLoS One 6, e23808.
Bayliss, W.M., Starling, E.H., 1899. The movements and innervation of the small intestine. J. Physiol. Lond. 24, 99–143.
Chen, C., Fang, R., Davis, C., Maravelias, C., Sibley, E., 2009. Pdx1 inactivation restricted to the intestinal epithelium in mice alters duodenal gene expression in enterocytes and enteroendocrine cells. Am. J. Physiol. Gastrointest. Liver Physiol. 927, 1126–1137.
Coles-Takabe, B., Brain, I., Purpura, K.A., Karpowicz, P., Zandstra, P.W., Morshead, C.M., van der Kooy, D., 2008. Don't look: growing clonal versus nonclonal neural stem cell colonies. Stem Cells 26, 2938–2944.
Costa, M., Brookes, S.J.H., Hennig, G.W., 2000. Anatomy and physiology of the enteric nervous system. Gut 47, iv15–iv19.
Danielian, P.S., Muccino, D., Rowitch, D.H., Michael, S.K., McMahon, A.P., 1998. Modification of gene activity in mouse embryos in utero by a tamoxifen-inducible form of Cre recombinase. Curr. Biol. 8, 1323–1326.
Druckenbrod, N.R., Epstein, M.L., 2005. The pattern of NC advance in the cecum and colon. Dev. Biol. 287, 125–133.
Durbec, P.L., Larsson-Blomberg, L.B., Schuchardt, A., Costantini, F., Pachnis, V., 1996. Common origin and developmental dependence on c-ret of subsets of enteric and sympathetic neuroblasts. Development 122, 349–358.
Edlund, H., 1999. Pancreas: how to get there from the gut? Curr. Opin. Cell Biol. 11, 663–668.
Edlund, H., 2002. Pancreatic organogenesis-developmental mechanisms and implications for therapy. Nat. Rev. Genet. 3, 524–532.
Engert, S., Liao, W.P., Burtscher, I., Lickert, H., 2009. Sox17-2A-iCre: a knock-in mouse line expressing Cre recombinase in endoderm and vascular endothelial cells. Genesis 47, 603–610.
Espinosa-Medina, I., Jevans, B., Boismoreau, F., Chettouh, Z., Enomoto, H., Muller, T., Birchmeier, C., Burns, A.J., Brunet, J.F., 2017. Dual origin of enteric neurons in vagal Schwan cell precursors and the sympathetic neural crest. Proc. Natl. Acad. Sci. 114, 11980–11985.
Estrada-Mondaca, S., Carreon-Rodriguez, A., Belkind-Gerson, J., 2007. Biology of the adult enteric neural stem cell. Dev. Dyn. 236, 20–32.
Fontaine, J., Le Douarin, N.M., 1977. Analysis of endoderm formation in the avian blastoderm by the use of quail-chick chimaeras. The problem of the neurectodermal origin of the cells of the APUD series. J. Embryol. Exp. Morphol. 41, 209–222.
Furness, J.B., Costa, M., 1980. Types of nerves in the enteric nervous system. Neuroscience 5, 1–20.
Gannon, M., Herrera, P.L., Wright, C.V., 2000. Mosaic Cre-mediated recombination in pancreas using the pdx-1 enhancer/promoter. Genesis 26, 143–144.
Gu, G., Dubauskaite, J., Melton, D.A., 2002. Direct evidence for the pancreatic lineage: NGN3+ cells are islet progenitors and are distinct from duct progenitors. Development 129, 2447–2457.
Guz, Y., Montminy, M.R., Stein, R., Leonard, J., Gamer, L.W., Wright, C.V., Teitelman, G., 1995. Expression of murine STF-1, a putative insulin gene transcription factor, in

cells of pancreas, duodenal epithelium and pancreatic exocrine and endocrine progenitors during ontogeny. Development 121, 11–18.
Herbarth, B., Pingault, V., Bondurand, N., Kuhlbrodt, K., Hermans-Borgmeyer, I., Puliti, A., Lemort, N., Goossens, M., Wegner, M., 1998. Mutation of the Sry-related Sox10 gene in dominant megacolon,a mouse model for human Hirschsprung disease. Proc. Natl. Acad. Sci. USA 95, 5161–5165.
Heuckeroth, R.O., 2018. Hirschsprung disease – integrating basic science and clinical medicine to improve outcomes. Nat. Rev. Gastroenterol. Hepatol. 15, 152–167.
Hirschsprung, H., 1888. Stuhlträgheit Neugeborener in Folge von dilatation und Hypertrophie des colons. Jahrb. Kinderheilkd. Phys. Erzieh. (Berl.) 27, 1–7.
Honig, G., Liou, A., Berger, M., German, M.S., Tecott, L.H., 2010. Precise pattern of recombination in serotonergic and hypothalamic neurons in a Pdx1-cre transgenic mouse line. J. Biomed. Sci. 17, 82.
Hotta, R., Anderson, R.B., Kobayashi, K., Newgreen, D.F., Young, H.M., 2010. Effects of tissue age, presence of neurones and endothelin-3 on the ability of enteric neurone precursors to colonize recipient gut: implications for cell-based therapies. Neurogastroenterol. Motil. 22, 338–e86.
Jinno, H., Morozova, O., Jones, K.L., Biernaskie, J.A., Paris, M., Hosokawa, R., Rudnicki, M.A., Chai, Y., Rossi, F., Marra, M.A., Miller, F.D., 2010. Convergent genesis of an adult neural crest-like dermal stem cell from distinct developmental origins. Stem Cells 28, (2027distinc).
Jonsson, J., Carlsson, L., Edlund, T., Edlund, H., 1994. Insulin-promoter-factor 1 is required for pancreas development in mice. Nature 371, 606–609.
Kawaguchi, Y., Cooper, B., Gannon, M., Ray, M., MacDonald, R.J., Wright, C.V.E., 2002. The role of the transcriptional regulator Ptf1a in converting intestinal to pancreatic progenitors. Nat. Genet 32, 128–134.
Kruger, G.M., Mosher, J.T., Bixby, S., Joseph, N., Iwashita, T., Morrison, S., J., 2002. NC stem cells persist in the adult gut but undergo changes in self-renewal, neuronal subtype potential, and factor responsiveness. Neuron 35, 657–669.
Le Douarin, N.M., 1969. Details of the interphase nucleus in Japanese quail (Coturnix coturnix japonica). Bull. Biol. Fr. Belg. 103, 435–452.
Le Douarin, N.M., Dupin, E., 1993. Cell lineage analysis in NC ontogeny. J. Neurobiol. 24, 146–161.
Lei, J., Howard, M.J., 2011. Targeted deletion of Hand2 in enteric neural precursor cells affects its functions in neurogenesis, neurotransmitter specification and gangliogenesis, causing functional aganglionosis. Development 138, 4789–4800.
Li, H., Cho, S.N., Evans, C.M., Dickey, B.F., Jeong, J., DeMayo, F.G., 2008. Cre-mediated recombination in mouse clara cells. Genesis 46, 300–307.
Lioubinski, O., Müller, M., Wegne, M., Sander, M., 2003. Expression of Sox transcription factors in the developing mouse pancreas. Dev. Dyn. 227, 402–408.
Mujtaba, T., Mayer-Proschel, M., Rao, M.S., 1998. A common neural progenitor for the CNS and PNS. Dev. Biol. 200, 1–15.
Nagy, A., 2000. Cre recombinase: the universal reagent for genome tailoring. Genesis 26, 99–109.
Nakanishi, N., Renfer, E., Technau, U., Rentzsch, F., 2012. Nervous systems of the sea anemone Nematostella vectensis are generated by ectoderm and endoderm and shaped by distinct mechanisms. Development 139, 347–357.
Pearse, A.G., 1982. Islet cell precursors are neurones. Nature 295, 96–97.
Pearse, A.G., Polak, J.M., 1971. NC origin of the endocrine polypeptide (APUD) cells of the gastrointestinal tract and pancreas. Gut 12, 783–788.
Perera, H.K., Caldwell, M.E., Hayes-Patterson, D., Teng, L., Peshavaria, M., Jetton, T.L., Labosky, P.A., 2006. Expression and shifting subcellular localization of the transcription factor, Foxd3, in embryonic and adult pancreas. Gene Expr. Patterns 6, 971–977.
Pictet, R.L., Rall, L.B., Phelps, P., Rutter, W.J., 1976. The neural crest and the origin of the insulin-producing and other gastrointestinal hormone-producing cells. Science 191, 191–192.
Roberts, R.R., Ellis, M., Gwynne, R.M., Bergner, A.J., Lewis, M.D., Beckett, E.A., Bornstein, J.C., Young, H.M., 2010. The first intestinal motility patterns in fetal mice are not mediated by neurons or interstitial cells of Cajal. J. Physiol. 588, 1153–1169.
Sang, Q., Young, H.M., 1996. Chemical coding of neurons in the myenteric plexus and external muscle of the small and large intestine of the mouse. Cell Tissue Res. 284, 39–53.
Schäfer, K.H., Saffrey, M.J., Burnstock, G., Mestres-Ventura, P., 1997. A new method for the isolation of myenteric plexus from the newborn rat gastrointestinal tract. Brain Res. Brain Res. Protoc. 1, 109–113.
Seaberg, R.M., van der Kooy, D., 2002. Adult rodent neurogenic regions: the ventricular subependyma contains neural stem cells, but the dentate gyrus contains restricted progenitors. J. Neurosci. 22, 1784–1793.
Seaberg, R.M., van der Kooy, D., 2003. Stem and progenitor cells: the premature desertion of rigorous definitions. Trends Neurosci. 26, 125–131.
Seaberg, R.M., Smukle, r.S.R., Kieffer, T.J., Enikolopov, G., Asghar, Z., Wheeler, M.B., Korbutt, G., van der Kooy, D., 2004. Clonal identification of multipotent precursors from adult mouse pancreas that generate neural and pancreatic lineages. Nat. Biotechnol. 22, 1115–1124.
Shi, S.R., Chaiwun, B., Young, L., Cote, R.J., Taylor, C.R., 1993. Antigen retrieval technique utilizing citrate buffer or urea solution for immunohistochemical demonstration of androgen receptor in formalin-fixed paraffin sections. J. Histochem. Cytochem. 41, 1599–1604.
Smukler, S.R., Arntfield, M.E., Razavi, R., Bikopoulos, G., Karpowicz, P., Seaberg, R., Dai, F., Lee, S., Ahrens, R., Fraser, P.E., Wheeler, M.B., van der Kooy, D., 2011. The adult mouse and human pancreas contain rare multipotent stem cells that express insulin. Cell Stem Cell 8, 281–293.
Song, J., Xu, Y., Hu, X., Choi, B., Tong, Q., 2010. Brain expression of Cre recombinase driven by pancreas-specific promoters. Genesis 48, 628–634.
Srinivas, S., Watanabe, T., Lin, C.S., William, C.M., Tanabe, Y., Jessell, T.M., Costantini, F., 2001. Cre reporter strains produced by targeted insertion of EYFP and ECFP into the 2626 locus. BMC Dev. Biol. 1, 4.
Teng, L., Mundell, N.A., Frist, A.Y., Wang, Q., Labosky, P.A., 2008. Requirement for Foxd3 in maintenance of neural crest progenitors. Development 135, 1615–1624.
Tropepe, V., Sibilia, M., Ciruna, B.G., Rossant, J., Wagner, E.F., van der Kooy, D., 1999. Distinct neural stem cells proliferate in response to EGF and FGF in the developing mouse telencephalon. Dev. Biol. 208, 166–188.
Vult von Steyern, F., Martinov, V., Rabben, I., Njå, A., de Lapeyrière, O., Lømo, T., 1999. The homeodomain transcription factors Islet 1 and HB9 are expressed in adult alpha and gamma motoneurons identified by selective retrograde tracing. Eur. J. Neurosci. 11, 2093–2102.
Wei, Z., Angerer, R.C., Angerer, L.M., 2011. Direct development of neurons within foregut endoderm of sea urchin embryos. Proc. Natl. Acad. Sci. USA 108, 9143–9147.
Wicksteed, B., Brissova, M., Yan, W., Opland, D.M., Plank, J.L., Reinert, R.B., Dickson, L.M., Tamarina, N.A., Philipson, L.H., Shostak, A., et al., 2010. Conditional gene targeting in mouse pancreatic beta-Cells: analysis of ectopic Cre transgene expression in the brain. Diabetes 59, 3090–3098.
Yntema, C.L., Hammond, W.S., 1954. The origin of intrinsic ganglia of trunk viscera from vagal NC in the chick embryo. J. Comp. Neurol. 101, 515–541.
Young, H.M., Ciampoli, D., Hsuan, J., Canty, A.J., 1999. Expression of Ret-, p75(NTR)-, Phox2a-, Phox2b-, and tyrosine hydroxylase-immunoreactivity by undifferentiated NC-derived cells and different classes of enteric neurons in the embryonic mouse gut. Dev. Dyn. 216, 137–152.
Young, H.M., Hearn, C.J., Ciampoli, D., Southwell, B.R., Brunet, J.F., Newgreen, D.F., 1998. A single rostrocaudal colonization of the rodent intestine by enteric neuron precursors is revealed by the expression of Phox2b, Ret, and p75 and by explants grown under the kidney capsule or in organ culture. Dev. Biol. 202, 67–84.
Young, H.M., Bergner, A.J., Muller, T., 2003. Acquisition of neuronal and glial markers by neural crest-derived cells in the mouse intestine. J. Comp. Neurol. 456, 1–11.